Project title: Range-wide survey for Louisiana Pigtoe *Pleurobema riddellii and* Texas Heelsplitter *Potamilus amphichaenus*

Table of Contents **Page No.**

Task 1 A: Distributional surveys across the range of *P. amphichaenus* and *P. riddellii*, particularly at sites with historical low survey effort

Contributing authors: Kyle Sullivan, Christa Edwards, Brad Littrell, and Tim Bonner

Addresses:
BIO-WEST, Inc. San Marcos, Texas 78666 (KS, CE, BL)
Texas State University, Department of Biology/Aquatic Station, San Marcos, Texas 78666 (TB)

Principal Investigators: Brad Littrell and Tim Bonner

Email: blittrell@bio-west.com, TBonner@txstate.edu

Study objectives

The goal of this study was to contribute to a better understanding of the viability of Louisiana Pigtoe and Texas Heelsplitter populations to inform the U.S. Fish and Wildlife Service's Species Status Assessment (SSA) process and facilitate future monitoring and conservation actions. Specific research objectives for each species include: characterizing the current distribution and assessing habitat associations. We assessed river drainages previously identified in the Research Plan as 'high-priority' and 'moderate-priority', meaning that contemporary survey data were either limited or absent. The surveyed drainages included the San Jacinto River, Trinity River, and Red River drainages within eastern Texas and western Louisiana.

Methods

Survey Design

In 2021, a total of 41 high-priority sites were surveyed in San Jacinto River, Trinity River, and Red River drainages. In 2022, a total of 13 moderate-priority sites were surveyed in the San Jacinto River drainage (Figure 1). Qualitative surveys via timed visual/tactile search methods were utilized to efficiently assess occurrence of the target species. A qualitative survey approach is an efficient search method to establish a list of taxa, as well as increase the detection probability of rare species (Vaughn et al. 1997; Strayer and Smith 2003). At each site, surveyors searched within all available mesohabitat types, focusing mainly in areas with more suitable mussel habitat. After completion of each site, sampling effort was recorded in person-hours (p-h) in order to calculate catch-per-unit-effort (CPUE; mussels/p-h). In 2022, semi-quantitative surveys were employed at eight sites in the San Jacinto River drainage where Louisiana Pigtoe was previously known to occur. At each site, survey areas consisted of a 150- m^2 plot and were searched for a total of four person-hours. Mussels were collected by visual and tactile methods.

Upon completion of qualitative or semi-quantitative surveys, all mussels were identified to species, enumerated, and up to 25 individuals per species were measured to the nearest millimeter (mm). Common and scientific names follow the 2021 checklist of freshwater mussels of the United States and Canada, developed by the Freshwater Mollusk Conservation Society Bivalve Names Subcommittee (FMCS 2021), except for Trinity Pigtoe (*Fusconaia chunii*), which is recognized as Texas Pigtoe (*Fusconaia askewi*) by Texas Parks and Wildlife Department (TPWD). Lastly, habitat conditions at each site were characterized based on depth-velocity conditions, physical habitat, and/or water quality, using qualitative descriptions or quantitative measurements.

Data Analysis

Community composition and assemblage structure

Survey data from activities in 2021 and 2022 were presented using several statistical procedures. First, a summary of total sites surveyed, and person-hours searched are provided for each river system. Raw abundance and percent relative abundance were calculated for each species grouped by San Jacinto River tributaries, Trinity River tributaries, Little Cypress Bayou,

Bayou Dorcheat, and Bayou Pierre. Patterns in central tendency and variation of site-level species richness and CPUE were assessed among these five river drainage groups using boxplots.

Differences in mussel assemblage structure were assessed using multivariate community statistics. Rare species that occurred at <5% of sites were omitted from the following analyses to account for potential confounding effects of imperfect detection associated with the methods used for this study (Metcalfe-Smith et al, 2000; Smith 2006). For analysis, a distance matrix among sites was first computed using the Bray-Curtis dissimilarity index and based on square root transformed community data. A multi-response permutation procedure (MRPP) was then used to test whether assemblage structure differed among rivers ($\alpha = 0.05$). Lastly, mean Bray-Curtis dissimilarity was calculated and visualized among rivers with a dendrogram to identify potential hierarchical clustering. Since rivers grouped into three basin-level clusters, dissimilarity percentages were calculated to identify what species most contributed to differences in assemblage structure among major river drainages. All statistical analyses assessing community composition and assemblage structure were performed using the R (4.2) packages 'ggplot2' (Lin Pedersen 2022) and 'vegan' (Oksanen 2020).

Habitat associations

Multilevel regression models were used to assess habitat associations of Louisiana Pigtoe and Texas Heelsplitter. Due to limited observations of each species during sampling, data from other survey efforts were included for analysis (i.e., Sabine River and Neches River drainages; BIO-WEST, unpublished data). For Louisiana Pigtoe, a multilevel zero-inflated regression model was fitted to estimate relative abundance (counts/150 m^2), which was chosen to accommodate the detection of excess zeros relative to assumptions of Poisson distribution (Gelman and Hill 2007; Zuur et al. 2009). Relative abundance could not be estimated for Texas Heelsplitter due to high zero inflation and limited variation in count data, resulting in convergence problems or poor model fit. Therefore, a multilevel logistic regression model was fit to estimate likelihood of occurrence (i.e., likelihood of positive detection) (Gelman and Hill 2007).

Response variables were modeled as a function of water depth (m), near-bed velocity (m/s), and percent substrate composition (%) (i.e., fixed effects). River basin and sampling river discharge were also included as group-level predictors (i.e., random effects) to account for variation unexplained by the covariates modeled within river basins and flow conditions during the time of sampling (Gelman and Hill 2007). River discharge was calculated based on mean daily discharge data from USGS stream gages closest to each sample site, and was standardized based on long-term medians (cfs / Q50; 1970-2022). Model fit was assessed for both species based on conditional coefficient of determination (R^2), as well as root mean squared error (RMSE) for Louisiana Pigtoe relative abundance and log loss for Texas Heelsplitter. Uncertainty of fixed effects coefficients were assessed via parameter simulations (iterations = 1,000) to further examine model fit and estimate parameter bias (Gelman and Hill 2007). Fitted functions of marginal effects were visualized for influential habitat variables, defined as covariates with 90% Confidence Intervals (CI) that don't overlap with zero. All analyses associated with model fitting and evaluation were conducted using R (4.2) packages 'ggeffects' (Ludecke 2023a), 'ggplot' (Lin Pedersen 2022), 'glmmTMB' (Brooks 2023), 'parameters' (Ludecke 2023b), and 'performance' (Ludecke 2023c).

Results

Community composition and assemblage structure

Freshwater mussel surveys in summer 2021 were conducted at 41 sites for a total of 131 person-hours of search effort within San Jacinto River (n = 12 sites), Trinity River (n = 11 sites), and Red River (n = 18) drainages. In summer 2022, freshwater mussel surveys were conducted at 13 sites for a total of 43 person-hours of search effort within San Jacinto River drainage. Summaries of total sites and search effort surveyed per river system can be found in Table 1.

Survey efforts resulted in a total of 5,149 mussels represented by 22 genera and 29 species. Species richness ranged from 9 species in Trinity River tributaries to 21 species in Bayou Pierre (Table 2). Median species richness and CPUE per site was higher in Bayou Pierre (16 species; 71.3 mussels/p-h) compared to Bayou Dorcheat (9 species; 14.8 mussels/p-h), San Jacinto tributaries (6 species; 11.9 mussels/p-h), Little Cypress Bayou (6 species; 5.5 mussels/p-h), and Trinity River tributaries (1 species; 0.5 mussels/p-h) (Figure 2). Although catch rates in San Jacinto River tributaries were generally lower, CPUE exceeded 100 mussels/p-h at two sites in the East Fork San Jacinto River (Figure 2). Moreover, Lake Creek and East Fork San Jacinto River were the only systems where Louisiana Pigtoe was collected (n = 7 sites). Louisiana Pigtoe CPUE ranged from 0.25 to 3.75 mussels/p-h (median = 0.25) and represented 1.1% of community composition (Table 2). Shell lengths of Louisiana Pigtoe from San Jacinto River drainages ranged from 27 to 48 mm (median = 42, mode = 36). Although quantitative survey methods were not used to evaluate recruitment during this study, 29% of Louisiana Pigtoe collected were less than or equal to 36 mm. Additionally, gravid females were observed at three of the seven sites (43%) where Louisiana Pigtoe was collected. Gravid females were documented in late June in 2021 and early June in 2022. No Texas Heelsplitters were collected in rivers surveyed within their native range (i.e., Trinity River).

Mussel assemblage structure differed among select drainages, although Pimpleback and Bankclimber were consistently dominant. The most common species among river drainages were Texas Pigtoe (46.8%, San Jacinto River), Yellow Sandshell (68.6%, Trinity River), and

Bankclimber (17.1-38.8% abundance, Red River) (Table 2). Results from MRPP detected meaningful differences among rivers (A = 0.22, $p = 0.001$), with mean distances being greater between groups (0.79) than within groups (0.61). The mean Bray-Curtis distance dendrogram displayed 3 distinct clusters that were grouped by major river basin. Cluster 1 included Trinity River tributaries (Bedias Creek and Keechi Creek), cluster 2 included San Jacinto River tributaries (East Fork San Jacinto River, Lake Creek), and cluster 3 included Red River tributaries (Little Cypress Bayou, Bayou Dorcheat, Bayou Pierre) (Figure 3). Percent dissimilarity among clusters ranged from about 80 to 90%. Dissimilarity of cluster 1 with cluster 2 and 3 was mainly due to Yellow Sandshell dominating assemblages in Trinity basin tributaries (11-14%). Cluster 2 differences were based on assemblages being dominated by Pimpleback (17-29%) and Texas Pigtoe (15-20%), whereas cluster 3 assemblages were more even in composition and exhibited a greater representation of Bankclimber (12-17%) and Threeridge (6-8%) (Table 2).

Habitat associations

Data used to fit habitat association models were based on observations from San Jacinto drainages (n = 8) for Louisiana Pigtoe and from Neches (n = 24) and Sabine (n = 28) drainages for both species. Goodness-of-fit indices demonstrated that variation in response variables were reliably estimated from the fitted models and that the Louisiana Pigtoe model ($R^2 = 0.92$, RMSE = 5.94) exhibited higher performance than the Texas Heelsplitter model ($R^2 = 0.63$, Log Loss = 0.39). Moreover, parametric bootstrapping showed minimal levels of bias when comparing parameters from the observed data versus simulated data. Model performance and bootstrapping results support that both models adequately represented the data generation process for Louisiana Pigtoe relative abundance and Texas Heelsplitter occurrence likelihood (Table 3 and 4).

Habitat variables identified as important predictors of Louisiana Pigtoe relative abundance included percent gravel, percent clay, and near-bed velocity. Effect size (estimate ± 90% CI) was highest for gravel (1.17 ± 0.56). The fitted function showing marginal effects of gravel displayed a curvilinear relationship. Relative abundance increased from about 0-10 mussels as gravel increased from 0 to 60%. The rate of change was more substantial from about 60 to 80% gravel, with relative abundance increasing from about 10 to 20 mussels (Figure 3). Effect size was similar between percent clay (0.50 ± 0.31) and near-bed velocity (0.50 ± 0.37) (Table 3). Fitted functions for these variables were more linear relative to percent gravel. Relative abundance was estimated to increase from 2 to 12 mussels as clay composition increased 0 to 40%. Relative abundance varied less with increasing near-bed velocity compared to percent gravel and clay, increasing from about 1 to 6 mussels as velocity increased from 0.0 to 0.50 m/s (Figure 4).

No habitat variables were identified as important predictors of Texas Heelsplitter likelihood of occurrence based on their 90% CIs overlapping with zero. Covariates with the smallest amount of CI overlap included percent clay and near-bed velocity. Effect sizes were similar for both covariates, but were positive for percent clay (1.15 ± 1.40) and negative for near-bed velocity (-1.01 ± 1.11) (Table 4). Occurrence likelihood was estimated to increase from about 20 to 50% as clay increased from 0 to 10%. It then increased to around 99% when clay composition rose to about 35%. For near-bed velocity, occurrence likelihood decreased from about 40 to 0% as velocity increased from 0.0 to 0.50 m/s (Figure 5).

Synthesis

This study aimed to improve understanding of the viability of Louisiana Pigtoe and Texas Heelsplitter populations and to facilitate future monitoring and conservation actions. Louisiana

Pigtoe is historically known from the Sabine, Neches-Angelina, Trinity, San Jacinto, and Red River drainages in Texas (Strecker 1931, Howells et al. 1996). During this study, Trinity, San Jacinto, and Red River drainages were surveyed, and Louisiana Pigtoe was only observed in one drainage. We collected a total of 31 live Louisiana Pigtoe at 32% of sites within San Jacinto River drainage. Results indicate that Louisiana Pigtoe currently persists in the East Fork San Jacinto River within Liberty County downstream of FM 2090 and Harris County near FM 1485. Additionally, Louisiana Pigtoe was observed in Lake Creek, a tributary to West Fork San Jacinto River, in Montgomery County upstream of Egypt. While there are historic reports of Louisiana Pigtoe in Lake Creek (OSUM_34911), recent occurrence within the West Fork San Jacinto River sub-basin was unknown prior to these surveys (Randklev et al. 2020).

Size structure of Louisiana Pigtoe from San Jacinto River drainage was dominated by size classes of about 40 mm. Although quantitative surveys were not used to assess recruitment, presence of smaller Louisiana Pigtoe (≤ 36 mm) suggests that recruitment is occurring within the San Jacinto River drainage. Additionally, gravid females were observed at three of the seven sites where Louisiana Pigtoe was collected, which were all documented in June. No Louisiana Pigtoe were collected in Trinity River or Red River drainages, despite previous records (Ford et al. 2016, Randklev et al. 2010, Strecker 1931). The status of Louisiana Pigtoe in Trinity River is unknown, but recent records between 2014-2016 indicate a few Louisiana Pigtoe individuals have been observed in the upper Trinity River and in Big Cypress Creek and Little Cypress Creek (Ford 2016). Although there were a few instances of field-identified Wabash Pigtoes *Fusconaia flava* in Bayou Dorcheat and Bayou Pierre appearing similar to Louisiana Pigtoe, we are awaiting genetic results to confirm the identification of these individuals. Multilevel model results suggested percent gravel, percent clay, and near-bed velocity were important predictors of

Louisiana Pigtoe relative abundance, which all exhibited a positive effect size. This suggests that Louisiana Pigtoe are more associated with fluvial habitats that have a greater prevalence of hydraulically stable substrates, which aligned with past observations in the Neches River (Burlakova et al. 2012; Troia et al. 2015). In contrast, previous surveys in Bayou Anacoco observed the species in fluvial habitats dominated by sand, though high prevalence of large woody debris was suggested to enhance hydraulic stability (Randklev et al. 2013).

Texas Heelsplitter is historically known from the Sabine, Neches-Angelina, and Trinity drainages (Strecker 1931, Howells et al. 1996). Previous records suggest Texas Heelsplitter occurs in the mainstem Trinity River (Randklev et al. 2017). This study focused survey efforts on Trinity River tributaries and no Texas Heelsplitters were observed. Multilevel model results failed to detect importance predictors of Texas Heelsplitter occurrence likelihood. Covariates with the lowest estimate uncertainty included percent clay and near-bed velocity, which displayed positive and negative effect sizes, receptively. Positive associations with percent clay suggests this substrate type provides hydraulic stability within habitats occupied by Texas Heelsplitter that often contain higher composition of sand and silt. The negative relationship between occurrence and near-bed velocity aligned with previous research and supports that Texas Heelsplitter are more associated with lentic habitats (Randklev et al. 2017; Walters et al. 2017). However, marginal effects of near-bed velocity did not result in occurrence likelihood >50%. This functional relationship suggests Texas Heelsplitter are associated with lentic habitats, but indicated that other factors, such as interactive effects of covariates used or predictors not included in the model, have a greater influence on their occurrence. More data with positive detections would likely provide more conclusive model-based inferences and refine current insights into habitat associations of Texas Heelsplitter.

References

Brooks, M. 2023. glmmTMB: Generalized Linear Mixed Models using Template Model Builder. R package version 1.1.7. https://www.rdocumentation.org/packages/glmmTMB

Burlakova, L.E., and A.Y. Karatayev. 2012. State-wide assessment of unionid diversity in Texas. Final Performance Report submitted to Texas Parks and Wildlife Department, Austin, Texas.

(FMCS) Freshwater Mollusk Conservation Society. 2021. The 2021 checklist of freshwater mussels (Mollusca: Bivalvia: Unionidae) of the United States and Canada. Appendix_1_Bivalves_Revised_Names_List_20210825.pdf (molluskconservation.org)

Ford, N.B., et al. 2016. Final Report, Endangered Species Research Projects for Freshwater Mussels, Region 2, East Texas, Texas Comptroller of Public Accounts. University of Texas at Tyler, Tyler, Texas.

Gelman, A., and J. Hill. 2007. Data Analysis Using Regression and Multilevel/Hierarchical Models. Cambridge University Press, New York, New York.

Howells, R.G. 1996. Info-Mussel Newsletter. Texas Parks and Wildlife Department-Inland Fisheries Heart of the Hills Research Station. Issue 3, 70 pp.

Kurth, J., C. Loftin, J. Zydlewski, and J. Rhymer. 2007. PIT tags increase effectiveness of freshwater mussel recaptures. Freshwater Science 26:253-260.

Lin Pedersen, T. 2022. ggplot2: Create Elegant Data Visualizations Using the Grammar of Graphics. R package version 3.3.6. https://rdocumentation.org/packages/ggplot2

Ludecke, D. 2023a. ggeffects: Estimated Marginal Means and Adjusted Predictions from Regression Models. R package version 1.2.1. https://www.rdocumentation.org/packages/ggeffects

Ludecke, D. 2023b. parameters: Processing of Model Parameters. R package version 0.21.0. https://www.rdocumentation.org/packages/parameters

Ludecke, D. 2023c. performance: Assessment of Regression Models Performance. R package version 0.10.3. https://www.rdocumentation.org/packages/performance

Oksanen, J. 2017. vegan: Community Ecology Package. R package version 2.4.2. https://www.rdocumentation.org/packages/vegan

Pollock, K.H. 1982. A capture-recapture design robust to unequal probability of capture. Journal of Wildlife Management 46:752–757.

Pollock, K.H., J.D. Nichols, C. Brownie, and J.E. Hines. 1990. Statistical inference for capture-recapture experiments. Wildlife Monographs 107: 3-97.

Randklev, C.R., S. Wolverton, B.J. Lundeen, and J.H. Kennedy. 2010. A paleozoological perspective on Unionid (Mollusca: Unionidae) zoogeography in the upper Trinity River basin. Ecological Applications 20:2359-2368.

Randklev, C.R., J. Skorupski, B. Lundeen, and E.T. Tsakiris. 2013. New distributional records for four rare species for freshwater mussels (Family: Unionidae) in southwestern Louisiana. Southeastern Naturalist 58:268-273.

Randklev, C.R., K. Inoue, M. Hart, and A. Pieri. 2017. Assessing the Conservation Status of Native Freshwater Mussels (Family: Unionide) in the Trinity River Basin. Natural Resources Institute, Texas A&M University, Dallas, Texas.

Randklev, C.R., N.B. Ford, M. Fisher, R. Anderson, C.R. Robertson, M. Hart, J. Khan, and R. Lopez. 2020. Mussels of Texas Project Database, Version 1.0.

Read, L.B., and K.H. Oliver. 1953. Notes of the ecology of the freshwater mussels of Dallas County. Field and Laboratory 21:75-80.

Sotola, V.A, K.T. Sullivan, B.M. Littrell, N.H. Martin, D.S. Stich, and T.H. Bonner. 2021. Short-term responses of freshwater mussels to floods in a southwestern U.S.A. river estimated using mark-recapture sampling. Freshwater Biology 66:346-361.

Strayer, D.L., and D.R. Smith. 2003. A Guide to Sampling Freshwater Mussel Populations. American Fisheries Society Monograph 8, Bethesda, Maryland.

Strecker, J.K. 1931. The Naiades or Pearly Freshwater Mussels of Texas. Baylor University Museum Special Bulletin 2:1-71.

Troia, M.J., L.R. Williams, M.G. Wiliams, and N.B. Ford. 2015. The process domains concept as a framework for fish and mussel habitat in a coastal plain river of southeastern North America. Ecological Engineering 75:484-496.

(USFWS) U.S. Fish and Wildlife Service. 2020. Draft--Species status assessment report for two freshwater mussels: Louisiana Pigtoe (*Pleurobema riddellii*) and Texas Heelsplitter (*Potamilus amphichaenus*). Version 1.1. Region 2, Albuquerque.

USFWS. 2023. Endangered and Threatened Wildlife and Plants; Endangered Species Status with Critical Habitat for Texas Heelsplitter, and Threatened Status with Section 4(d) Rule and Critical Habitat for Louisiana Pigtoe. Federal Register 88:16776-16832.

Vaughn, C.C., C.M. Taylor, and K.J. Eberhard. 1997. A comparison of the effectiveness of timed searches vs. quadrat sampling in mussel surveys. Conservation and Management of Freshwater Mussels II: Proceedings of a UMRCC Symposium.

Walters, A.D., et al. 2015. High-resolution ecological niche modeling of threatened freshwater mussels in east Texas, USA. Aquatic Conservation: Marine and Freshwater Ecosystems 27:1251-1260.

Watters, G.T., M.A. Hoggarth, and D.H. Stansbery. 2009. The Freshwater Mussels of Ohio. The Ohio State University, Columbus, Ohio.

Young, S. P., and J.J. Isely. 2008. Evaluation of methods for attaching PIT tags and biotelemetry devices to freshwater mussels. Molluscan Research 28:175-178.

Zurr, A.F., E.N. Ieno, N.J., Walker, A.A. Saveliev, and G.M. Smith. 2009. Mixed Effects Models and Extensions in Ecology with R. Springer Science and Business Media, New York, New York.

Table 1. Summary of total sites and person-hours searched within all east Texas and western Louisiana river systems surveyed for freshwater mussels in summer 2021 and 2022.

	2021		2022	
River System	**Total Sites**	**Total Person-hours**	**Total Sites**	**Total Person-hours**
San Jacinto River				
Caney Creek	2	4	-	-
East Fork San Jacinto River	7	27	8	32
Lake Creek	2	15	5	11
West Fork San Jacinto River	1	2	-	-
Trinity River				
Bedias Creek	4	11	-	-
Big Creek	1	2	-	-
Boggy Creek	1	2	-	-
Catfish Creek	1	2	-	-
Long King Creek	1	2	-	-
Lower Keechi Creek	1	2	-	-
Menard Creek	1	2	-	-
Upper Keechi Creek	1	3	-	-
Red River				
Bayou Dorcheat	7	28	-	-
Bayou Pierre	7	20	-	-
Little Cypress Bayou	4	9	-	-
Total	**41**	**131**	**13**	**43**

Table 2. Raw abundance (#) and percent relative abundance (%) for mussel species collected during summer 2021 and 2022 surveys in east Texas and western Louisiana river drainages. Common names follow FMCS (2021), except for Trinity Pigtoe, which is recognized as Texas Pigtoe by TPWD.

Species	**San Jacinto River Tributaries**		**Trinity River Tributaries**		**Little Cypress Bayou**		**Bayou Dorcheat**		**Bayou Pierre**	
	#	**%**	**#**	**%**	**#**	**%**	**#**	**%**	**#**	**%**
Threeridge	13	0.4	0	0.0	3	5.0	11	2.2	264	16.3
Rock Pocketbook	0	0.0	0	0.0	0	0.0	0	0.0	43	2.6
Wartyback	0	0.0	0	0.0	0	0.0	0	0.0	18	1.1
Pimpleback	1,258	43.5	5	7.1	9	15.0	26	5.2	113	7.0
Texas Pigtoe	1,356	46.8	0	0.0	0	0.0	0	0.0	0	0.0
Wabash Pigtoe	0	0.0	0	0.0	3	5.0	79	15.8	25	1.5
Round Pearlshell	0	0.0	0	0.0	0	0.0	0	0.0	4	0.2
Louisiana Fatmucket	15	0.5	3	4.3	8	13.3	16	3.2	87	5.4
Sandbank Pocketbook	1	0.0	0	0.0	0	0.0	0	0.0	0	0.0
Yellow Sandshell	51	1.8	48	68.6	4	6.7	42	8.4	77	4.7
Little Spectaclecase	4	0.1	0	0.0	0	0.0	2	0.4	0	0.0
Washboard	15	0.5	0	0.0	2	3.3	4	0.8	136	8.4
Threehorn Wartyback	0	0.0	0	0.0	0	0.0	0	0.0	54	3.3
Bankclimber	102	3.5	0	0.0	17	28.3	194	38.8	277	17.1
Louisiana Pigtoe	31	1.1	0	0.0	0	0.0	0	0.0	0	0.0
Fragile Papershell	9	0.3	0	0.0	4	6.7	5	1.0	12	0.7
Bleufer	16	0.6	0	0.0	0	0.0	5	1.0	38	2.3
Giant Floater	0	0.0	2	2.9	2	3.3	1	0.2	2	0.1
Mapleleaf	2	0.1	2	2.9	5	8.3	7	1.4	232	14.3
Pondmussel	0	0.0	0	0.0	0	0.0	15	3.0	0	0.0
Creeper	3	0.1	0	0.0	0	0.0	5	1.0	0	0.0
Texas Lilliput	1	0.0	6	8.6	1	1.7	18	3.6	4	0.2
Gulf Mapleleaf	0	0.0	1	1.4	0	0.0	0	0.0	80	4.9
Pistolgrip	0	0.0	2	2.9	2	3.3	58	11.6	107	6.6
Fawnsfoot	0	0.0	0	0.0	0	0.0	0	0.0	5	0.3
Deertoe	18	0.6	0	0.0	0	0.0	0	0.0	43	2.6
Tapered Pondhorn	0	0.0	1	1.4	0	0.0	0	0.0	0	0.0
Pondhorn	0	0.0	0	0.0	0	0.0	12	2.4	0	0.0
Paper Pondshell	0	0.0	0	0.0	0	0.0	0	0.0	3	0.2
Species Richness	**16**		**9**		**12**		**17**		**21**	
Total Abundance	**2895**		**70**		**60**		**500**		**1624**	

Table 3. Parameter estimates from the multilevel zero-inflated regression model used to estimate relative abundance of Louisiana Pigtoe. Performance indices and parameter bias estimates (estimated - simulated) are also provided, which represent goodness-of-fit and uncertainty of parameter estimates, respectively. Parameters marked with (*) denote covariates identified as important predictors of the response, defined as having 90% confidence intervals not overlapping with zero.

Parameter	**Estimate**	**90% CI**	**Parameter Bias**
Count Model			
Intercept	0.64	2.12	-0.01
standard dev. (basin)	2.19	-	-
Water depth	0.15	0.51	0.00
Near-bed velocity*	0.50	0.37	0.01
% clay*	0.50	0.31	0.00
% sand	-0.23	0.51	-0.02
% gravel*	1.17	0.56	-0.02
% cobble	0.13	0.27	0.00
Zero-inflated model			0.00
Intercept	0.05	0.73	0.14
standard dev. (basin)	< 0.001	-	-
standard dev. (river discharge)	0.99	-	-
R^2	0.92		
RMSE	5.94		

Table 4. Parameter estimates from the multilevel logistic regression model used to estimate occurrence likelihood of Texas Heelsplitter. Performance indices and parameter bias estimates (estimated - simulated) are also provided, which represent goodness-of-fit and uncertainty of parameter estimates, respectively.

Parameter	**Estimate**	**90% CI**	**Parameter Bias**
Intercept	-1.37	2.09	-0.03
standard dev. (basin)	1.63	-	-
standard dev. (river discharge)	0.39	-	-
Water depth	0.25	0.73	0.01
Near-bed velocity	-1.01	1.11	0.00
% clay	1.15	1.40	0.01
% silt	-0.61	1.47	0.02
% sand	-0.73	1.25	0.02
% cobble	-0.20	1.41	0.05
R^2	0.63		
Log loss	0.39		

Figure 1. Location of sampling sites during 2021 and 2022 freshwater mussel survey efforts in San Jacinto River, Trinity River, and Red River drainages.

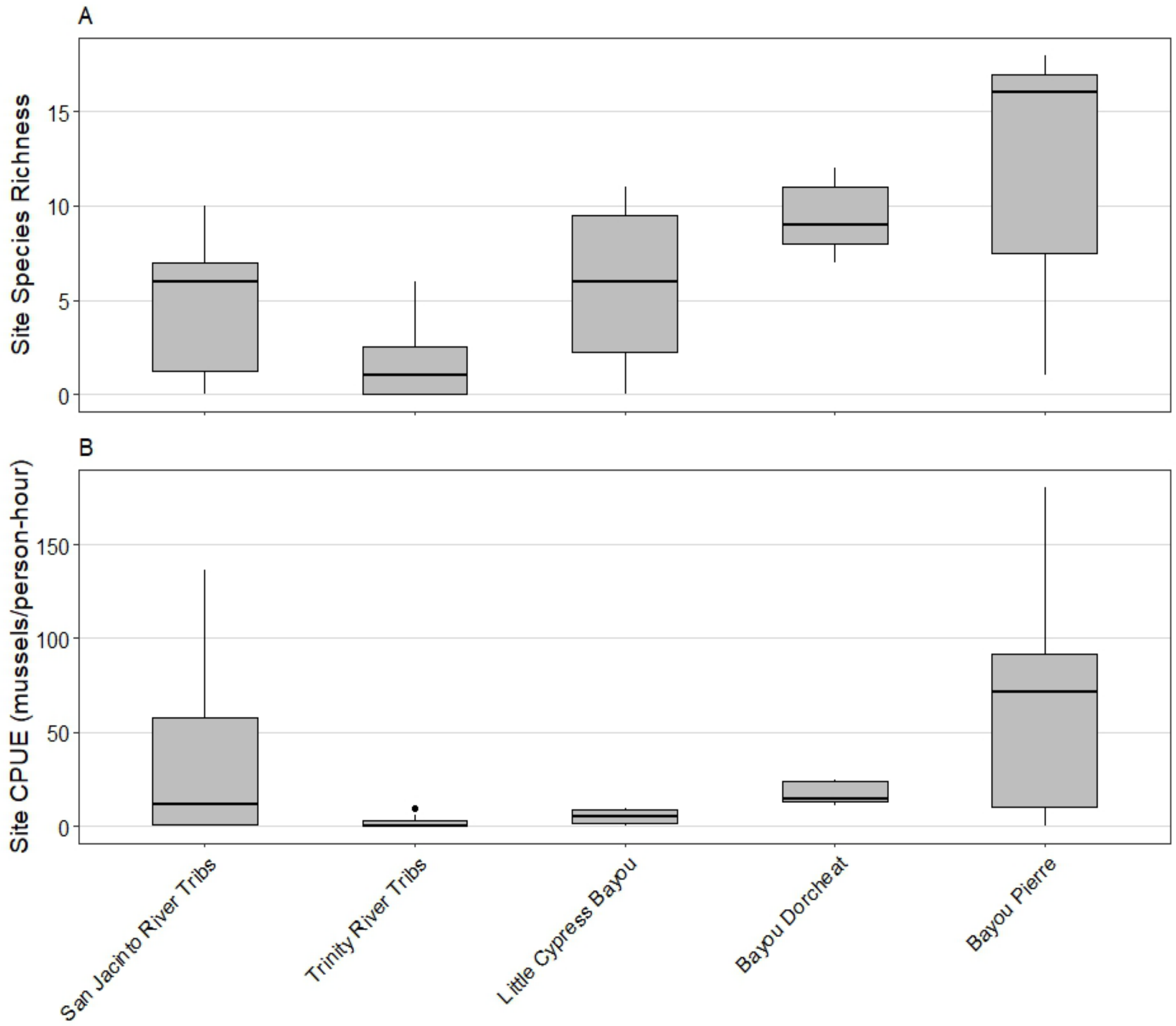

Figure 2. Boxplots displaying freshwater mussel species richness (A) and catch-per-unit-effort (CPUE; B) by site among east Texas and western Louisiana river drainages surveyed in summer 2021 and 2022. The thick horizontal line in each box is the median and the upper/lower bounds of each box represents the interquartile range. Whiskers represent minimum/maximum values up to 1.5 times the interquartile range and outliers beyond this are designated with solid black circles.

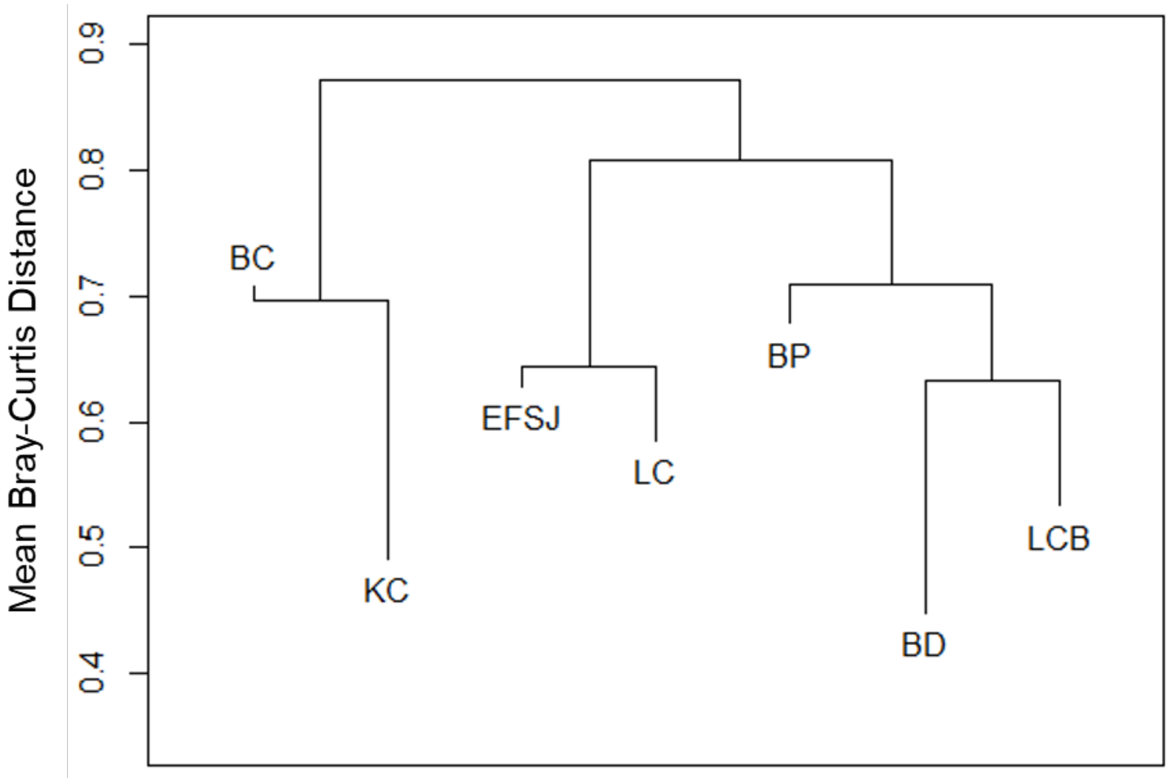

Figure 3. Dendrogram displaying mean Bray-Curtis distances between 7 rivers and creeks within San Jacinto River, Trinity River, and Red River drainages. Rivers and creeks assessed include Lake Creek (LC), East Fork San Jacinto River (EFSJ), Bedias Creek (BC), Keechi Creek (KC), Little Cypress Bayou (LCB), Bayou Dorcheat (BD), and Bayou Pierre (BP).

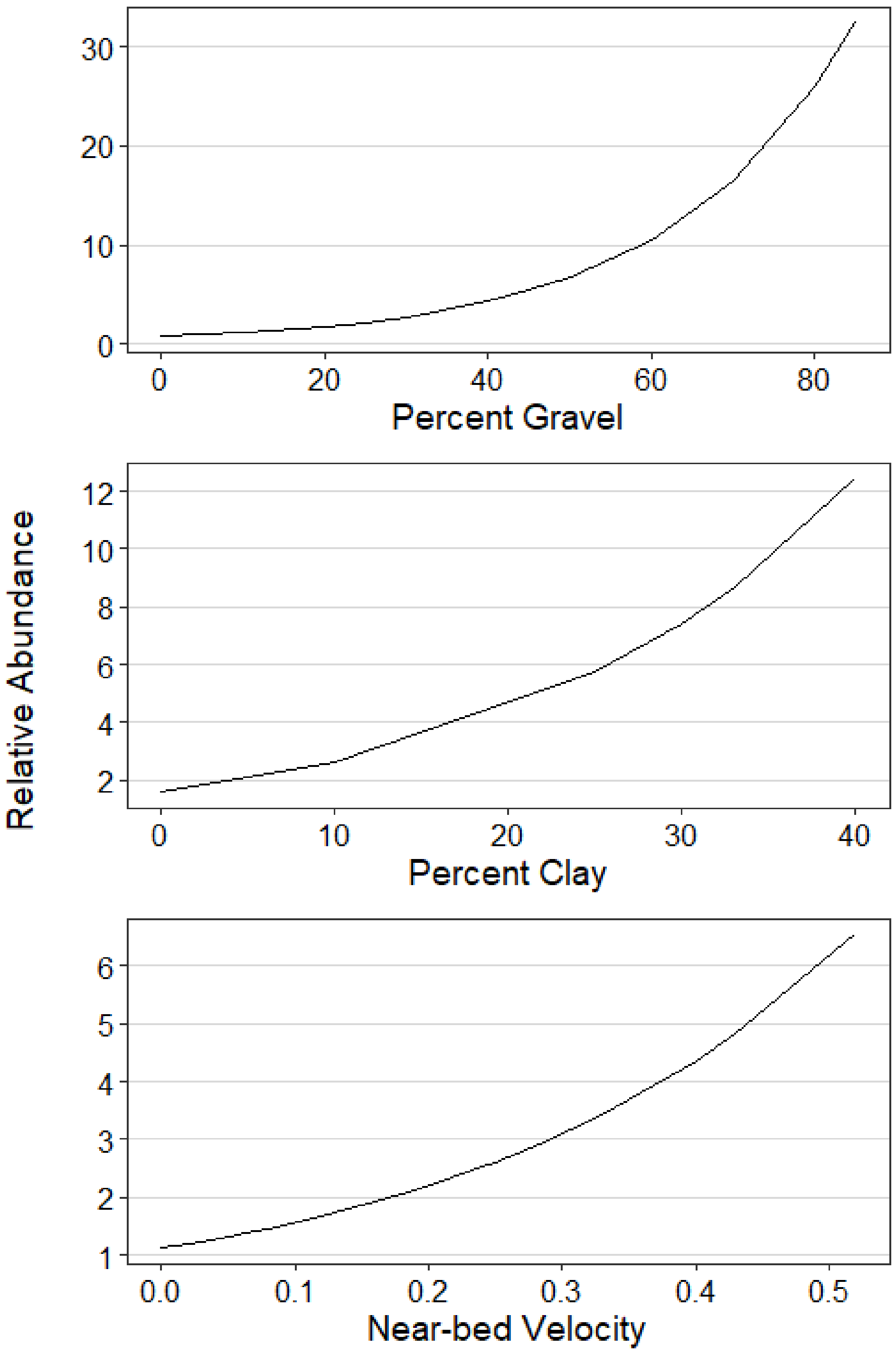

Figure 4. Predicted relative abundance of Louisiana Pigtoe as a function of percent gravel (%, top panel), percent clay (%, middle panel) and near-bed velocity (m/s, bottom panel). Predictions are based on marginal effects estimates, which adjusts predictions by holding other model covariates constant at their mean effect size.

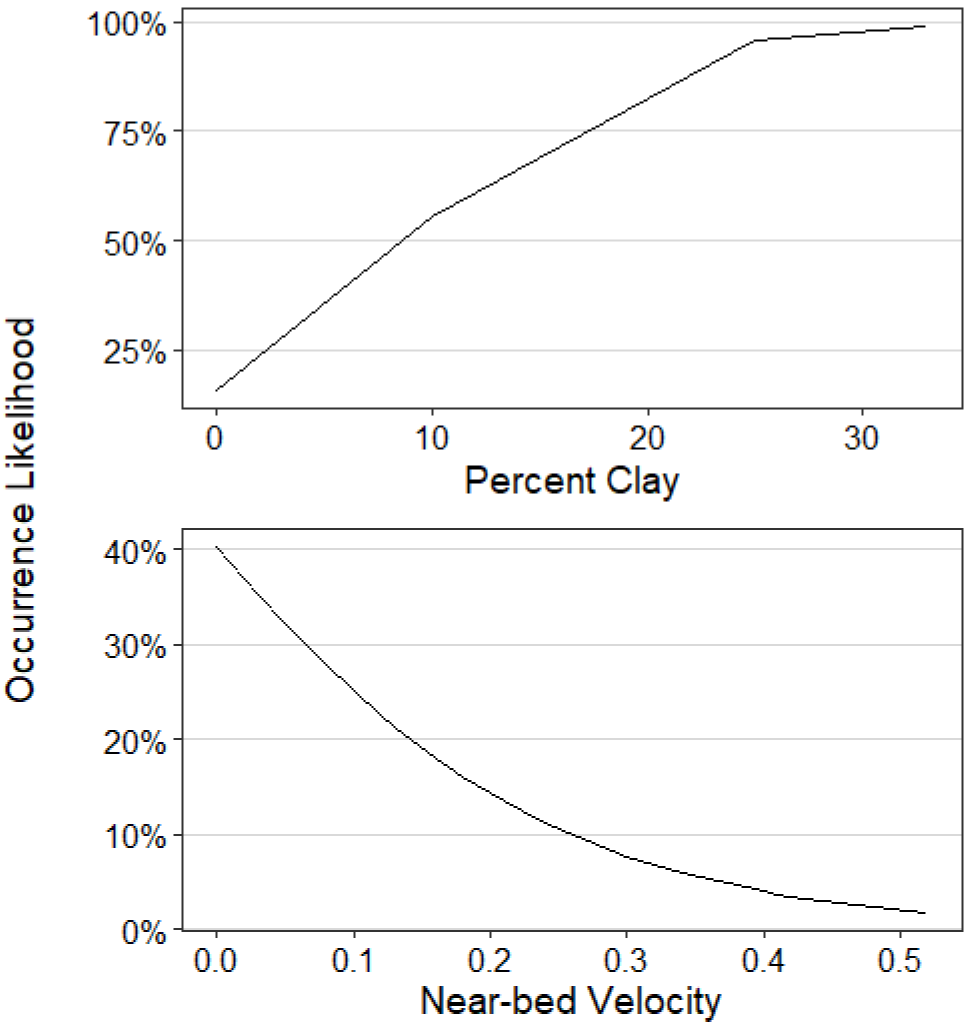

Figure 5. Predicted occurrence likelihood of Texas Heelsplitter as a function of percent clay (%, top panel) and near-bed velocity (m/s, bottom panel). Predictions are based on marginal effects estimates, which adjusts predictions by holding other model covariates constant at their mean effect size.

Task 1 B: B.A. Steinhagen surveys and analysis

Contributing Authors: Brad Littrell and Christa Kunkel

Address:
BIO-WEST, Inc. San Marcos Texas 78666

Principal Investigator: Brad Littrell

Email: blittrell@bio-west.com

Study objectives

In 2019, the U.S. Army Corp of Engineers (USACE) lowered B.A. Steinhagen reservoir approximately 5.5 m in order to complete dam maintenance and safety inspections. During the 31-day drawdown period, Texas Parks and Wildlife Department (TPWD) biologists documented a total of 4,203 freshwater mussels from 21 species, including 72 state-threatened and ESA-candidate Texas Heelsplitter *Potamilus amphichaenus*. Additional observations by Lower Neches Valley Authority (LNVA) staff during this drawdown period suggested Texas Heelsplitter to be common in certain desiccated portions of the reservoir. Based on this information, B.A. Steinhagen likely harbored the largest known population of Texas Heelsplitter.

Since the reservoir was refilled in 2019, there is no freshwater mussel survey data available. Therefore, dive surveys were planned in June 2023 to evaluate if freshwater mussels, specifically Texas Heelsplitter, had recolonized portions of the reservoir since the 2019 drawdown. Additionally, if documented, growth rates of Texas Heelsplitter could be estimated over the approximately 4-year period since the 2019 drawdown. Furthermore, since another reservoir drawdown was conducted in July 2023 immediately following the dive surveys, survey transects were revisited following desiccation to allow for quantification of dive survey efficiency. It should be noted that freshwater mussels are known to exhibit species-specific behavioral responses to dewatering and desiccation. Some species move laterally to avoid desiccation, some are known to burrow, and some species can close tightly and survive short periods of desiccation (Gough et al. 2012). As a result, post-dewatering data may not represent exactly what was present during dive surveys. However, examining community composition and species abundance between dive surveys and post-dewatering surveys may help to elucidate patterns in species response and detectability.

Methods

BIO-WEST, Inc. (BIO-WEST) conducted freshwater mussel dive surveys June 29-30, 2023 within B.A. Steinhagen Reservoir. The surveys were focused on 10 locations where Texas Heelsplitter were found during the 2019 drawdown. At each location, georeferenced transects of lead-core rope with a buoy on each end were established for divers to follow while conducting the surveys. Scientific divers using SCUBA gear worked in pairs, with each diver surveying a path along one side of the transect rope. Transects were 25 or 50 meters long and the width of the search area was adjusted so that the total search area for each transect was approximately 100 m^2. All collected mussels were placed in mesh bags and brought to the surface for identification, enumeration, and measurement (each mussel was measured to the nearest mm shell length) by a trained malacologist. Each divers survey time was noted to allow quantification of catch-per-unit-effort (CPUE). After data collection, all mussels were returned to the transect of origin alive.

Crews revisited the 10 survey transects following the drawdown of B.A. Steinhagen Reservoir on July 13-14, 2023. GPS coordinates were used to return to the same exact survey areas and collect all live or freshly dead mussels. Mussels were identified, measured, and enumerated, as before. These data were used to compare mussel community composition and density between dive surveys and post-dewatering surveys, and therefore, assess survey efficiency and patterns in species detectability.

Results and Discussion

During dive surveys on June 29-30, 2023, 837 mussels representing 19 species were collected. Transect depths ranged from 1.5 to 4 m. Substrates were dominated by silt or sand with limited gravel. Among the dive surveys, the most abundant species were Pimpleback *Cyclonaias pustulosa* (31%), Gulf Mapleleaf *Tritogonia nobilis* (20%), Bankclimber *Plectomerus dombeyanus* (16%), and Threehorn Wartyback *Obliquaria reflexa* (14%) (Table 1). During the post-dewatering survey on July 13-14, 2023, a total of 1,449 mussels representing 20 species were collected. The most abundant species were Bankclimber (34%), Pimpleback (21%), and Threehorn Wartyback (10%) (Table 1). One previously undetected species, Louisiana Fatmucket *Lampsilis hydiana* (n=1), was observed during the post-dewatering survey. Texas Heelsplitter was collected during both the dive and post-dewatering surveys. During the dive survey, one 100-mm Texas Heelsplitter was collected in Transect 5. In contrast, 41 Texas Heelsplitter were collected in eight out of the 10 transects during the post-dewatering survey. Sizes of the collected Texas Heelsplitter ranged from 16 to 118 mm. Additionally, crews from LNVA surveyed a larger portion of the dewatered reservoir and collected a total of 72 Texas Heelsplitter, ranging in size from 21 to 131 mm. The abundance and size range of Texas Heelsplitter collected suggest that recolonization has been occurring since the reservoir was desiccated during the 2019 dewatering and that B.A. Steinhagen likely still harbored one of the largest known populations of Texas Heelsplitter. Length frequency histograms suggest that Texas Heelsplitter can reach sizes of up to 131 mm within approximately four years (Figure 1).

Median mussel density was higher in the post-dewatering transects (1.38 mussels/m^2; range: 0.41 - 4.32 mussels/m^2) than in the dive survey transects (0.79 mussels/m^2; range: 0.11 - 1.92 mussels/m^2) (Figure 2). Likewise, median species richness was higher in the post-dewatering transects (12 species/transect; range: 8 - 16 species/transect) than in the dive survey transects (9.5 species/transect; range 6 - 11 species/transect) (Figure 3). If potential movement of mussels to and from transects is ignored between June and July surveys and the number collected during post-dewatering surveys is assumed to represent the total number of mussels present during dive surveys, 58% of mussels were detected in the dive surveys (Table 1). Species with high detection rates in the dive surveys included Deertoe *Truncilla truncata* (100%), Flat Floater *Utterbackiana suborbiculata* (100%), Pimpleback (85%), Giant Floater *Pyganodon grandis* (81%), and Threehorn Wartyback (79%) (Table 1), suggesting these species are efficiently detected by surveyors. Species with low detection in the dive surveys included Louisiana Fatmucket (0%), Texas Heelsplitter (2%), and Paper Pondshell *Utterbackia imbecillis* (4%). All these taxa are relatively thin shelled and mobile species, and reduced detection in dive surveys may be influenced by movement during dewatering, or by burrowing post-dewatering. In contrast to other species, there was greater detection of Mapleleaf *Quadrula quadrula* and Pistolgrip *Tritogonia verrucossa* in the dive surveys than there was in the post-dewatering surveys (Table 1). Both species are highly sculptured, and therefore, may be more easily detected by surveyors using tactile methods. These species may also have burrowed into the mud following dewatering and thus avoided detection during post-dewatering surveys.

Reference

Gough, H. M., A. M. Gascho Landis, and J. A. Stoeckel. 2012. Behaviour and physiology are linked in the responses of freshwater mussels to drought. Freshwater Biology (2012) 57:2356-2366. doi:10.1111/fwb.12015

Table 1. Abundance and percent relative abundance of freshwater mussels observed among dive surveys and post-dewatering surveys and percent of mussels observed in the post-dewatering surveys that were detected in the dive surveys.

Scientific Name	**Common Name**	**Dive Abundance**	**Dive % Abundance**	**Post-dewatering Abundance**	**Post-dewatering % Abundance**	**Difference**	**% Detected**
Amblema plicata	Threeridge	4	0.48	9	0.62	-5	44.44
Arcidens confragosus	Rock Pocketbook	1	0.12	5	0.35	-4	20.00
Cyclonais pustulosa	Pimpleback	259	30.94	303	20.91	-44	85.48
Lampsilis hydiana	Louisiana Fatmucket	0	0.00	1	0.07	-1	0.00
Lampsilis teres	Yellow Sandshell	9	1.08	38	2.62	-29	23.68
Megalonais nervosa	Washboard	5	0.60	13	0.90	-8	38.46
Obliquaria reflexas	Threehorn Wartyback	115	13.74	145	10.01	-30	79.31
Plectomerus dombeyanus	Bankclimber	135	16.13	496	34.23	-361	27.22
Potamilus amphichaenus	Texas Heelsplitter	1	0.12	41	2.83	-40	2.44
Potamilus fragilus	Fragile Papershell	17	2.03	100	6.90	-83	17.00
Potamilus purpuratus	Bleufer	30	3.58	81	5.59	-51	37.04
Pyganodon grandis	Giant Floater	21	2.51	26	1.79	-5	80.77
Quadrula quadrula	Mapleleaf	54	6.45	24	1.66	30	225.00
Toxolasma texasiense	Texas Lilliput	4	0.48	7	0.48	-3	57.14
Tritogonia nobilis	Gulf Mapleleaf	6	0.72	57	3.93	-51	10.53
Tritogonia verrucosa	Pistolgrip	170	20.31	70	4.83	100	242.86
Truncilla donaciformis	Fawnsfoot	2	0.24	4	0.28	-2	50.00
Truncilla truncata	Deertoe	2	0.24	2	0.14	0	100.00
Utterbackia imbecillis	Paper Pondshell	1	0.12	26	1.79	-25	3.85
Utterbackiana suborbiculata	Flat Floater	1	0.12	1	0.07	0	100.00
	Total	**837**		**1449**			**57.76**
	Species Richness	**20**		**21**			**95.23**

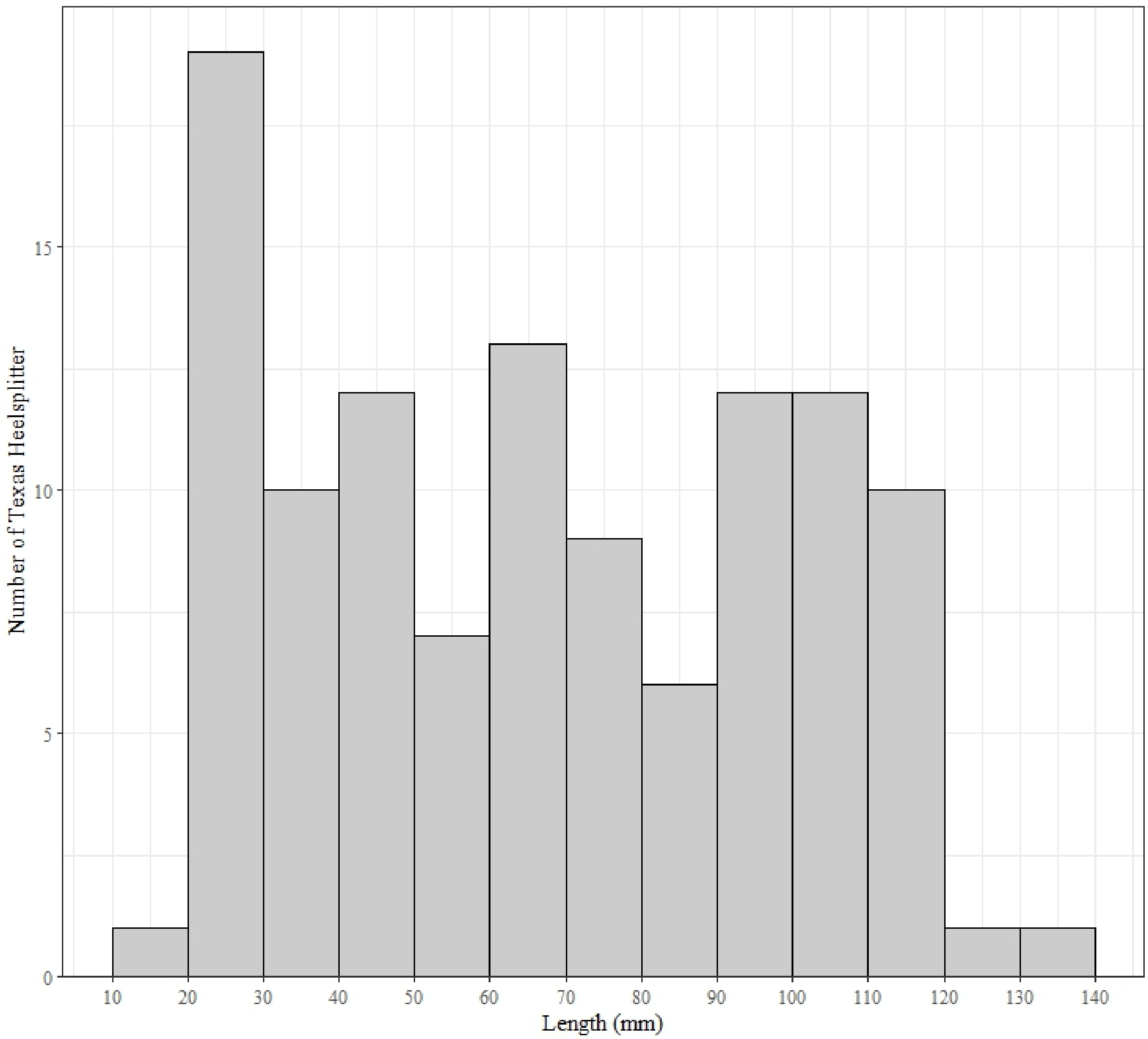

Figure 1. Shell lengths of Texas Heelsplitter collected during the dive (n=1), post-dewatering (n=41), and LNVA (n=72) surveys.

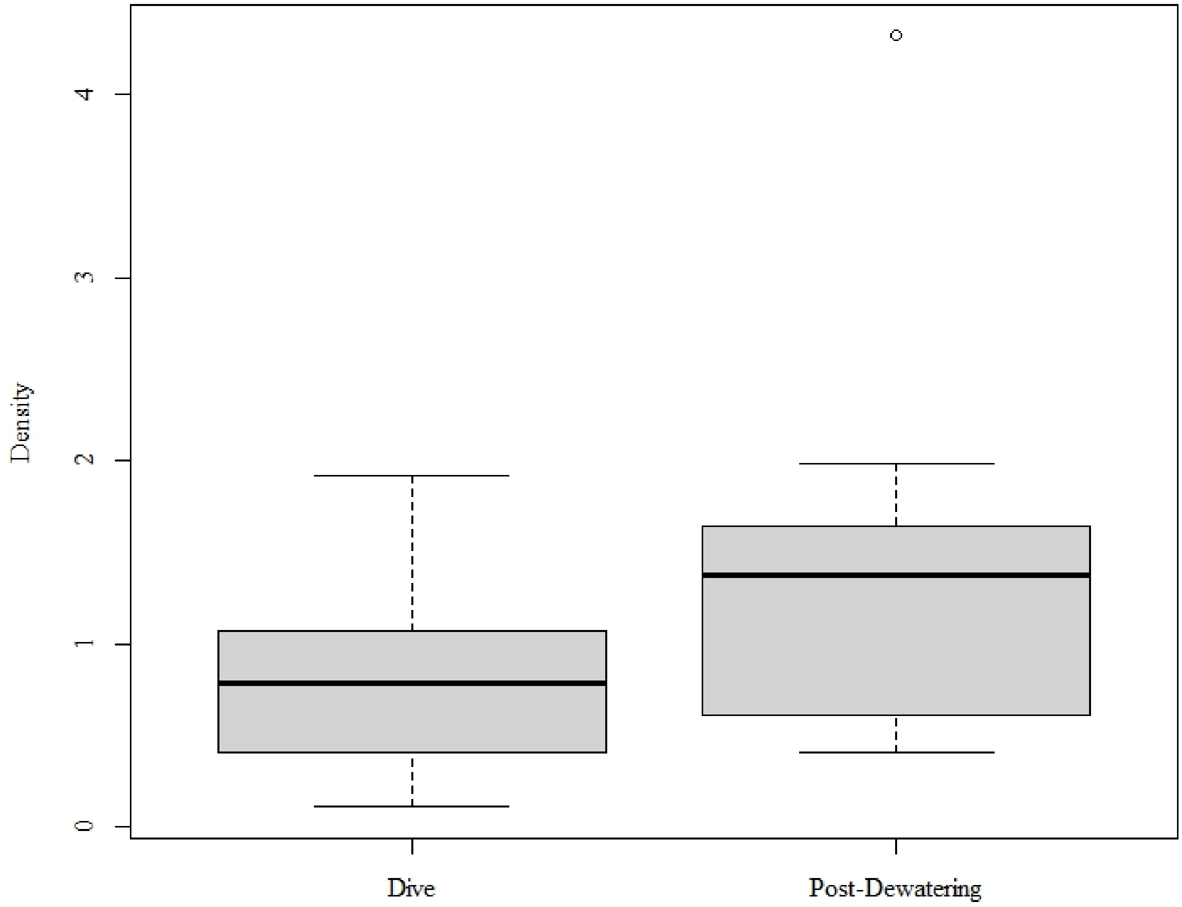

Figure 2. Boxplots displaying differences in mussel densities observed in the dive and post-dewatering surveys in summer 2023. The thick horizontal line in each box is the median and the upper/lower bounds of each box represent the interquartile range.

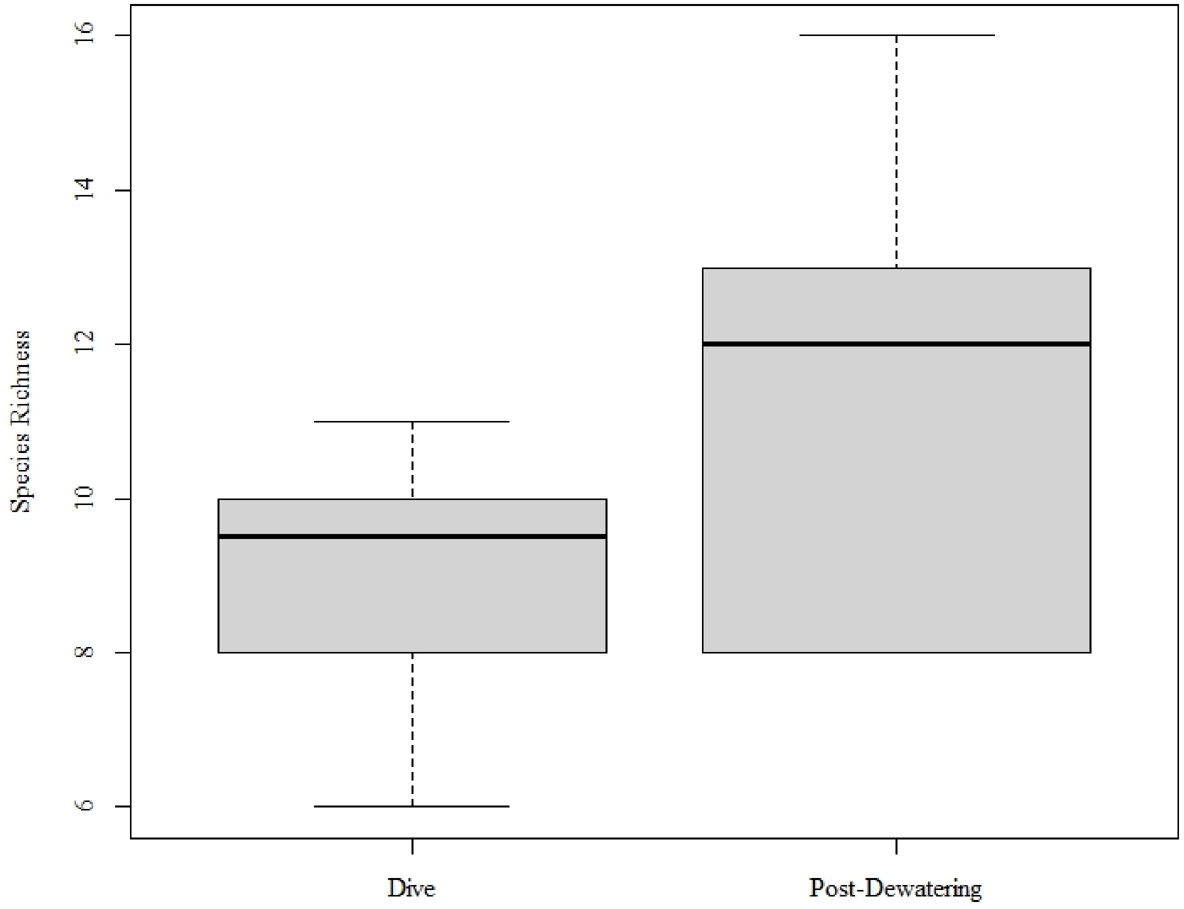

Figure 3. Boxplots displaying differences in mussel species richness observed in the dive and post-dewatering surveys in summer 2023. The thick horizontal line in each box is the median and the upper/lower bounds of each box represent the interquartile range.

Task 1 C: Mussel and fish communities within off-channel habitats of the lower Neches River and lower Sabine River basins

Contributing Authors: Eli Leal, Ovi Saldana, Alex Zalmat, Christa Kunkel, Brad Littrell, Noland Martin, and Tim Bonner

Addresses:
Texas State University, Department of Biology, San Marcos, Texas 78666
BIO-WEST, Inc. San Marcos, Texas 78666

Principal Investigator: Tim Bonner and Brad Littrell

Email: TBonner@txstate.edu and blittrell@bio-west.com

Study objectives

Objectives of this study were to quantify mussel and fish communities within off-channel habitats of the lower Neches River and lower Sabine River basins. Particular emphasis was on the Texas Heelsplitter *Potamilus amphichaenus*. From previous collections by U.S. Fish and Wildlife Service (2020), Texas Heelsplitter inhabits mainstem rivers, smaller tributaries, and reservoirs. During a 2019 dewatering event in B.A. Steinhagen Reservoir (Tyler and Jasper counties, Neches River basin), an abundant population of Texas Heelsplitter was documented, suggesting that Texas Heelsplitter might be more abundant in lentic-type environments (e.g., reservoirs, off-channel habitats) than in mainstem rivers and smaller tributaries.

Methods

Five off-channel water bodies were sampled within the lower Neches River basin on the Angelina River (1 site) and Neches River (4 sites) with sites spanning a distance of 140 river-km, and five off-channel water bodies were sampled on the lower Sabine River with sites spanning a distance of 20 river-km (Table 1). In addition to selecting water bodies along a longitudinal gradient, we selected off-channel water bodies that were connected during low flow with the river mainstem. Connection with the river mainstem increased the likelihood of recent migrates of mussels and fish, suggested recently formed oxbows, and enabled public access through the river mainstem.

Within the Neches River basin, Sites 1 and 2 were sampled on August 10 - 11, 2022, sites 3, 4, and 5 were sampled September 16 – 17, 2022. At each site, two experimental gill nets were set and allowed to fish for 0.5 day. At sites 1 and 2, numerous American Alligator *Alligator mississippiensis* were observed along with extensive damages in the experimental gill nets, presumably because of American Alligators becoming entangled in the nets. Extensive damages to the nets greatly decreased the efficiency of gill nets, and the nets could possibly injure non-targeted aquatic fauna. Consequently, gill nets were not set at sites 3, 4, and 5. Boat-mounted electrofishing equipment was used to sample 60 to 100% of the shoreline habitat. Multiple seine hauls, using a standard seine (3 m × 1.8 m, mesh size = 3.2 mm) or bag seine (5 m × 1.8 m, mesh size = 3.2 mm), were made in wadeable habitats (i.e., near shore, open water, when available). Available wadeable habitats were sampled exhaustively until no new species were captured. Mussel surveys consisted of 4 person-hour tactile searches in each off-channel habitat using mask and snorkel and/or dive gear.

Within the lower Sabine River, sites 6 – 10 were sampled March 12 – 13, 2023 using electroshocking and gill nets as described for the Neches River basin. However, Sabine River flows were elevated (>15,000 cfs, median flow = 14,800, period of record: 1960 – 2023; USGS Station 08030500), which precluded efficient fish sampling with seines or mussel sampling. Seining and mussel sampling was conducted at Sites 6 – 10 during July 18 – 19, 2023 at lower flows (1,500 cfs, median flow = 5,200, period of record: 1960 – 2023).

Results

Mussel community

Twenty-three mussel species and 1,629 individuals were observed among the five off-channel habitats in the lower Neches River basin (Table 2). Mapleleaf *Quadrula quadrula* was the most abundant species (28% in relative abundance), followed by Gulf Mapleleaf *Tritogonia nobilis* (23%), and Bankclimber *Plectomerus dombeyanus* (14%). Catch per unit effort (CPUE) of mussels ranged from 1 mussel/person hour (p-hr) at Site 2 to 180 mussels/p-hr at Site 3. Mean CPUE (± 1 SE) was 81.6 (38.24) mussels/p-hr. Texas Heelsplitter *Potamilus amphichaenus* ranked 14th in abundance (0.74% in relative abundance) and were taken from Site 3 (N = 3), Site 4 (N = 7), and Site 5 (N = 2). Mean CPUE (± 1 SE; range) of Texas Heelsplitter was 0.6 (0.32; 0 – 1.75) mussels/p-hr.

Twenty mussel species and 1,792 individuals were observed among five off-channel habitats in the lower Sabine River. Round Pearlshell *Glebula rotundata* was the most abundant species (36% in relative abundance), followed by Yellow Sandshell *Lampsilis teres* (17%), and Gulf Mapleleaf (15%). Catch per unit effort of mussels ranged from 6.8 mussels/p-hr at Site 8 to 174 mussels/p-hr at Site 6. Mean CPUE (± 1 SE) was 89.8 (27.30) mussels/p-hr. Texas Heelsplitter was not observed from off-channel water bodies in the lower Sabine River.

Fish community

Fifty-six fish species and 3,493 individuals were observed across all gear types among the five off-channel habitats within the lower Neches River basin (Table 3). Bullhead Minnow *Pimephales vigilax* was the most abundant species (29% in relative abundance) followed by Mimic Shiner *Notropis volucellus* (6.6%) and Blacktail Shiner *Cyprinella venusta* (6.4%). The only confirmed fish host for Texas Heelsplitter is Freshwater Drum *Aplodinotus grunniens* (USFWS 2020). Freshwater Drums (N = 9; 0.26% in relative abundance, size range: 100 – 610 mm in total length) were taken from all sites except Site 1.

Fifty-one species and 6,140 individuals were observed across all gear types among the five off-channel habitats within the lower Sabine River. Weed Shiner was the most abundant species (30% in relative abundance) followed by Threadfin Shad *Dorosoma petenense* (16%) and Blacktail Shiner *Cyprinella venusta* (9.1%). Freshwater Drums (N = 2; 0.03% in relative abundance) were taken only from Site 6.

Synthesis

The expectation of Texas Heelsplitter being more abundant in off-channel water bodies was marginally supported in the lower Neches River basin. In this study, 12 Texas Heelsplitter were observed within 3 of 5 (60% occurrence) off-channel water bodies with a mean CPUE of 0.6 and a range of 0 to 1.75 mussels/p-hr. In a recent study in the upper Sabine River (Schoeck et al, In review), 7 Texas Heelsplitter were observed in 4 of 28 mainstem sites (14% occurrence) with a mean CPUE of 0.06 and range of 0 to 1 mussel/p-hr. Based on these findings, limited data suggest that off-channel water bodies might yield greater numbers of Texas Heelsplitter than surveys in mainstem rivers. Additional surveys of off-channel water bodies are planned for the upper Sabine River and upper Neches River and could provide further support for Texas Heelsplitter associations with off-channel water bodies.

Lower Sabine River is not within the reported occupied range of the Texas Heelsplitter (USFWS 2020). Consequently, lack of Texas Heelsplitter in off-channel water bodies within the lower Sabine River supports previous assessments.

References

Schoeck, C.N., K.T. Sullivan, J. Guajardo, B.M. Littrell, B. Kirby, A.W. Groeger, and T.H. Bonner. In review. Mussel community and changes in water quality within a southcentral river basin of North America with emphasis on two federally proposed species. American Malacological Bulletin.

(USFWS) US Fish and Wildlife Service, 2020. Draft--Species status assessment report for two freshwater mussels: Louisiana Pigtoe (*Pleurobema riddellii*) and Texas Heelsplitter (*Potamilus amphichaenus*). Version 1.1. Region 2, Albuquerque.

Table 1. Basin, off-channel water body type, coordinates, and approximate water body area (based on areal imagery) for 10 sites sampled August 2022 through July 2023.

Basin	Site	Habitat type	Lat/long	Area (m^2)
Neches	1	oxbow	30.9167, -94.1596	41,360
	2	oxbow	30.8956, -94.2017	83,575
	3	slough	30.4468, -94.1110	37,346
	4	oxbow	30.4357, -94.1148	26,253
	5	oxbow	30.1745, -94.1165	58,133
Sabine	6	slough	30.3851, -93.7612	43,047
	7	oxbow	30.3670, -93.7587	94,454
	8	oxbow	30.3587, -93.7613	36,982
	9	slough	30.3346, -93.7655	43,609
	10	slough	30.2973, -93.7309	7,994

Table 2. Species and relative abundances of mussels observed in 10 off-channel water bodies within the Neches River and Sabine River basins, August 2022 through July 2023.

Species	Common name	Neches basin	Sabine basin
Amblema plicata	Threeridge	1.6	0.28
Arcidens confragosus	Rock Pocketbook	0.43	0.11
Cyclonaias pustulosa	Pimpleback	1.3	1.6
Fusconaia askewi	Texas Pigtoe		0.39
Glebula rotundata	Round Pearlshell	3.5	36.2
Lampsilis hydiana	Louisiana Fatmucket	3.0	3.7
Lampsilis satura	Sandbank Pocketbook	0.12	
Lampsilis teres	Yellow Sandshell	6.1	17.1
Leaunio lienosa	Little Spectaclecase		0.17
Megalonaias nervosa	Washboard	4.8	0.17
Obliquaria reflexa	Threehorn Wartyback	5.6	0.33
Plectomerus dombeyanus	Bankclimber	13.5	7.4
Pleurobema riddellii	Louisiana Pigtoe	0.06	
Potamilus amphichaenus	Texas Heelsplitter	0.74	
Potamilus fragilis	Fragile Papershell	1.8	0.17
Potamilus purpuratus	Bleufer	3.2	0.28
Pyganodon grandis	Giant Floater	0.98	3.2
Quadrula quadrula	Mapleleaf	28.4	10.5
Toxolasma texasiense	Texas Lilliput	0.06	3.2
Tritogonia nobilis	Gulf Mapleleaf	23.0	14.5
Tritogonia verrucosa	Pistolgrip	0.43	0.39
Truncilla truncata	Deertoe	0.12	
Uniomerus tetralasmus	Pondhorn	0.67	
Utterbackia imbecillis	Paper Pondshell	0.06	0.06
Utterbackiana suborbiculata	Flat Floater		0.28
Rangia cuneata	Rangia Clam	0.55	
	Total (N)	1,632	1,795
	Species Richness	23	20

Table 3. Species and relative abundances of fishes observed across all gear types in 10 off-channel water bodies within the Neches and Sabine River basins, August 2022 through July 2023.

Species	Common name	Neches basin	Sabine basin
Ichthyomyzon castaneus	Chestnut Lamprey		0.02
Atractosteus spatula	Alligator Gar	0.03	
Lepisosteus oculatus	Spotted Gar	1.3	0.28
Lepisosteus osseus	Longnose Gar	0.92	0.33
Amia calva	Bowfin	0.03	0.03
Dorosoma cepedianum	Gizzard Shad	2.8	0.78
Dorosoma petenense	Threadfin Shad	5.4	15.6
Anchoa mitchilli	Bay Anchovy	6.2	
Cyprinus carpio	Common Carp	0.03	0.05
Cyprinella lutrensis	Red Shiner	2.7	
Cyprinella venusta	Blacktail Shiner	6.4	9.1
Hybopsis amnis	Pallid Shiner	0.49	0.02
Hybognathus nuchalis	Mississippi Silvery Minnow		0.02
Lythrurus fumeus	Ribbon Shiner		1.0
Macrhybopsis hyostoma	Shoal Chub	0.57	
Notemigonus crysoleucas	Golden Shiner		0.07
Notropis texanus	Weed Shiner	0.46	30.1
Notropis volucellus	Mimic Shiner	6.6	1.0
Opsopoeodus emiliae	Pugnose Minnow	0.11	5.8
Pimephales vigilax	Bullhead Minnow	29.1	1.8
Carpiodes carpio	River Carpsucker	0.23	
Ictiobus cyprinellus	Bigmouth Buffalo	0.14	0.02
Ictiobus bubalus	Smallmouth Buffalo	3.3	0.50
Minytrema melanops	Spotted Sucker	0.40	0.11
Moxostoma poecilurum	Blacktail Redhorse		0.05
Ameiurus natalis	Yellow Bullhead	0.03	
Ictalurus furcatus	Blue Catfish	0.20	0.18
Ictalurus punctatus	Channel Catfish	0.37	0.10
Noturus gyrinus	Tadpole Madtom	0.06	
Pylodictis olivaris	Flathead Catfish	0.29	
Esox americanus	Redfin Pickerel	0.03	0.15
Aphredoderus sayanus	Pirate Perch	0.03	0.10
Mugil cephalus	Stripped Mullet	0.43	3.5
Menidia audens	Mississippi Silverside	0.97	0.29
Labidesthes sicculus	Brook Silverside	4.2	5.7
Fundulus blairae	Western Starhead Minnow	0.72	0.02
Fundulus chrysotus	Golden Topminnow	0.57	

Table 3 (continued). Species and relative abundances of fishes observed across all gear types in 10 off-channel water bodies within the Neches and Sabine River basins, August 2022 through July 2023.

Species	Common Name	Neches basin	Sabine basin
Fundulus notatus	Blackstripe Topminnow	3.1	1.2
Fundulus olivaceus	Blackspotted Topminnow		1.2
Gambusia affinis	Western Mosquitofish	1.9	2.7
Morone mississippiensis	Yellow Bass		0.03
Lepomis auritus	Redbreast Sunfish	0.54	
Lepomis gulosus	Warmouth	0.29	0.18
Lepomis humilis	Orangespotted Sunfish		0.08
Lepomis macrochirus	Bluegill Sunfish	3.9	5.6
Lepomis marginatus	Dollar Sunfish	0.06	0.07
Lepomis megalotis	Longear Sunfish	2.8	2.6
Lepomis microlophus	Redear Sunfish	1.5	0.16
Lepomis miniatus	Redspotted Sunfish	0.29	0.11
Lepomis sp	Juvenile Sunfish	5.3	3.7
Lepomis symmetricus	Bantam Sunfish	0.03	
Micropterus punctulatus	Spotted Bass	0.86	0.23
Micropterus salmoides	Largemouth Bass	1.7	0.81
Pomoxis annularis	White Crappie	0.83	0.29
Pomoxis nigromaculatus	Black Crappie	0.43	1.7
Etheostoma asprigene	Mud Darter		0.18
Etheostoma chlorosoma	Bluntnose Darter	0.06	2.26
Etheostoma fusiforme	Swamp Darter	0.03	0.02
Etheostoma gracile	Slough Darter		0.02
Etheostoma proeliare	Cypress Darter	0.03	0.05
Percina macrolepida	Bigscale Logperch	0.17	0.02
Percina sciera	Dusky Darter	0.03	
Percina shumardi	River Darter	0.06	
Aplodinotus grunniens	Freshwater Drum	0.26	0.03
Elassoma zonatum	Banded Pygmy Sunfish	0.06	
Trinectes maculatus	Hogchoker	0.40	0.07
	Total N	3,493	6,140
	Species Richness	55	51

Task 2: Mark-recapture study to assess population dynamics in *P. amphichaenus* and *P. riddellii* habitat and establish the study for long-term monitoring by stakeholders

Contributing authors: Daniel Stich and Brandon Guerrero

Addresses: 113A Perna Science, SUNY College at Oneonta, NY 13820

Principal Investigators: Daniel Stich

Email: daniel.stich@oneonta.edu

Study objectives

The objectives were to 1) establish two mark-recapture study sites in areas supporting sufficient numbers of Texas Heelsplitter (*Potamilus amphichaenus*) and Louisiana Pigtoe (*Pleurobema riddellii*), 2) repeat surveys in each location yearly, replicating a one sampling event for each of three secondary periods, and 3) assess accuracy and precision of estimates to determine the influence of numbers of mussels, sites, surveys, and species-specific detection probabilities.

Methods

Field Sites

The study sites chosen for mark-recapture surveys were in the Neches and Sabine Rivers (Figure 1). A YSI ProDSS multiprobe was used to record water quality parameters during each survey, including temperature, dissolved oxygen, and pH. Depth and velocity were recorded with the aid of an electromagnetic velocity meter and incremental wading rod. Substrate percent composition was visually estimated based on the modified Wentworth scale.

Mussel surveys

All mussel surveys were conducted under TPWD Scientific Collection Permit (#SPR-0101-131). A Biomark® HPR passive integrated transponder (PIT) reader was used to detect mussels tagged with PIT tags prior to conducting timed searches. Afterward, surveyors used a mask and snorkel to visually and tactilely sample for the mussels during timed searches. Plots were selected around areas where the target species (Texas Heelsplitter and Louisiana Pigtoe) were previously documented.

Initial tagging was conducted at two sites in the Neches River basin during October 5-6, 2021, and resampling was conducted three times at each site during August 2-4 2022. Initial tagging at Sabine River sites was conducted September 24 and 25 2020, with two primary recapture events in August 03 and 11-12, 2021, and September 20-22, 2022, each with three secondary sampling events. To maintain consistency in the estimates derived from analyses in the Neches River for this study, we collapsed the secondary events from the Sabine River into three primary events for this analysis.

The mussels found during the tactile search were brought back to processing tables where measurements were collected, and tags were applied or recorded if already tagged, after which they were promptly returned to the survey site. Shellfish tags (Hallprint) and passive integrated transponder (PIT) tags (Biomark) were affixed with cyanoacrylate glue. PIT tags were affixed to Texas Heelsplitter and Louisiana Pigtoe only.

Empirical survival analysis

Cormack-Jolly-Seber (CJS) models (Cormack 1964; Jolly 1965; Seber 1965) are a common framework for estimating recapture and survival probabilities of individuals or groups of organisms (see Kéry and Schaub 2012). The CJS model can be fit using multinomial (Lebreton et al. 1992), or state-space likelihood (Gimenez et al. 2007; Royle 2008). We used a state-space method, in a Bayesian framework, to estimate survival and detection probabilities.

Assumptions that need to be considered when using these models include those related to tag retention, accurate identification of individuals, random sampling of marked and unmarked individuals within the population, and population closure (i.e., no immigration or emigration). Tag loss can result in underestimation of survival, but Sotola et al. (2021) indicated minimal tag loss (< 2%) in several similar species in the Colorado River using the same protocols. If an individual is misidentified, it can cause bias if no corrections can be made. To account for this, we dropped any mussels from the data set that could not be reliably, individually identified. Each capture and recapture event are assumed to be random samples from the population to avoid biasing estimates that can result from sampling heterogeneity; therefore, mussels were sampled under similar environmental conditions at similar times of year for consistency. Finally, emigration is also confounded with mortality within this framework because an individual that emigrates can no longer be found in the study population, thus our estimates of survival represent "apparent" survival, and not "true" survival. While this cannot be accounted for directly within the CJS framework, additional years of data collection in the Neches River could be used to fit open-population models that can account for emigration and allow for estimation of true survival (e.g., Sotola et al. 2021).

Survival of tagged mussels was estimated using CJS mark-recapture models (Cormack 1964; Jolly 1965; Seber 1965). These models use observations of individual detection (1 or 0) on repeated sampling events to estimate survival (alive or dead) while accounting for detection probability (detected or not).

For this specific application, the true state (*z*) of individuals (*i*) during each sampling event *t* after the first was assumed to be the outcome of a Bernoulli process governed by the apparent survival probability during the preceding interval, φ_t:

$$z_{i,t} \sim \text{Bernoulli}(\varphi_{i,t}).$$

The observed state (*y*) of individuals during each sampling event was modeled as the outcome of a Bernoulli distribution, as a function of individual detection probability (p), conditioned on the true state $z_{i,t}$:

$$y_{i,t} \sim \text{Bernoulli}(p_{i,t}) \times z_{i,t}.$$

We used logit-scale priors for φ and p that allowed for incorporation of individual covariates on these parameters. Global means (hyperpriors) μ_φ and μ_p were drawn from normal distributions on the logit scale with a mean of zero and a variance of 1 (precision = $1/\sigma^2$):

$$\mu_\varphi \sim \text{Normal}(0, 1),$$

and

$$\mu_p \sim \text{Normal}(0, 1).$$

Hyperpriors on global variances (σ_φ^2 and σ_p^2) were drawn from uniform distributions with a minimum of 0 and a maximum of 10:

$$\sigma_{\varphi}^{2} \sim \text{Uniform}(0, 10),$$

and

$$\sigma_{p}^{2} \sim \text{Uniform}(0, 10).$$

For grouping variables (species or time), group-specific priors for $\varphi_{i,t}$ and $p_{i,t}$ were drawn from normal distributions with a means equal to μ_{φ} or μ_{p}, and variances equal to σ_{φ}^{2} and σ_{p}^{2}:

$$\text{logit}(\varphi_{i,t}) \sim \text{Normal}(\mu_{\varphi}, \sigma_{\varphi}^{2}),$$

and

$$\text{logit}(p_{i,t}) \sim \text{Normal}(\mu_{p}, \sigma_{p}^{2}).$$

All models were written and run in JAGS (Plummer 2003) using the R2jags package (Su and Yajima 2021) for R (R Core Team 2022) and estimated with Markov chain Monte Carlo (MCMC) methods. All models used 3 chains, 50,000 iterations, a burn-in of 40,000 iterations, and we retained every fifth sample to reduce autocorrelation, resulting in 3,000 samples from the posterior distribution of each model parameter. Convergence of the Markov chains was confirmed utilizing the Gelman-Rubin diagnostic for convergence (Gelman and Rubin 1992) and effective sample size (ESS) was >300 per chain per parameter. All data and code used for the empirical analysis are available (Data S1).

Multiple models that included time and species-specific parameterizations for survival and detection of the mussels were compared to determine the best supported structure using deviance information criterion (DIC). The model with the lowest DIC was considered to be the best supported model. Other models with a difference of < 2.00 in DIC (ΔDIC) compared to the best model were also considered to be well supported. First, we compared varying models of detection with effects of year, species, both or neither while holding survival constant across periods to ensure we accounted for variability in detection probability. After determining the best detection model structure, we used DIC to determine whether species-specific or time-specific survival were better supported. All models during this second phase of variable selection for the Neches River included time-varying survival because intervals between surveys varied in duration and a fundamental objective of the analysis was to estimate annual survival from the first full-year interval.

Simulation-based power analysis

We used empirical survival and detection probabilities from the Neches River mark-recapture study to assess study design constraints to accuracy and precision of estimates from Cormack-Jolly-Seber (CJS) models within a simulation framework. We used mean survival detection probabilities for the Texas Heelsplitter and Louisiana Pigtoe from the species-specific survival model from the Neches River to randomly generate individual capture histories. The true state (z, alive = 1, dead = 0) of simulated individuals (i) during each sampling event (t) was the outcome of a Bernoulli process dependent on survival in the previous interval, φ_t, conditional on the first capture:

$$z_{it} \sim \text{Bernoulli}(\varphi_{i,t}).$$

The observed state (y) of individuals during sampling events was modeled as conditional on the true state, $z_{\mathrm{i,t}}$, where the observation (1 = seen, 0 = not seen) was the outcome of a Bernoulli distribution as a function of detection probability (p):

$$y_{i,t} \sim \mathrm{Bernoulli}(\mathrm{p}_{i,t}) \times z_{i,t}.$$

A CJS model identical to the φ.p. model from the empirical analysis was then used to estimate $\hat{\varphi}$ and $\hat{\mathrm{p}}$ from the simulated capture histories. For each simulation, known values of φ and p were drawn from normal distributions on the logit scale based on empirical means and standard deviations. We evaluated accuracy and precision of model-estimated $\hat{\varphi}$ and $\hat{\mathrm{p}}$ relative to known values of φ and p across varying numbers of sampling periods, $\mathrm{T} \in (0, 5, \ldots, 50)$, and number of tagged individuals (sample size), $n \in (0, 10, \ldots, 500)$. Accuracy (error) was calculated as -$\hat{\varphi}$ - φ for each simulation, and precision was measured as the standard deviation of the posterior for $\hat{\varphi}$ for each simulation. The mean squared error of φ was calculated for each simulation to assess tradeoffs in accuracy and precision.

We ran all simulations through the University at Buffalo Center for Computational Research high-performance cluster. Simulation code was written in the open-source programming language R (R Core Team 2022), models were written in JAGS (Plummer 2003) and analyzed with R2jags (Su and Yajima 2021) in parallel through the snowfall package (Knauss 2022) using Markov chain Monte Carlo methods. For each model, we ran 3 Markov chains with 50,000 iterations each, a burn-in of 15,000, and we retained every fifth sample from the posterior to reduce autocorrelation between estimates. All code used for simulation-based power analysis are made available (Data S1).

Results

Environmental conditions

Water temperatures at the sites in the Neches River ranged from 28.1 to 33.5°C, dissolved oxygen ranged from 6.35 to 10.72 mg/L, and pH ranged from 8.48 to 8.86 during this study. In the Sabine River, water temperature ranged from 26.94 to 33.50°C, dissolved oxygen ranged from 6.35 to 10.72 mg/L, and pH ranged from 8.48 to 8.86 during mussel surveys. The lower and upper Neches River sites contained similar mixtures of substrates dominated by silt (~75%), clay (~20%), and sand (~5%). The Sabine site comprised a mixture of sand (~10-50%), gravel (~10-30%), cobble (20%), and bedrock (~20-50%).

Survey results

The total number of mussels tagged during the study was 3,840. A total of 2,081 individuals representing 22 species were detected across sites in the Neches River (Table 1). A total of 1,846 individuals in 20 species were tagged in the Sabine River (Table 2). One Texas Lilliput (*Toxolasma texasiense*) was collected in the Neches River but was not tagged or recaptured and was therefore dropped from counts (Table 1) and subsequent analyses. The total number of species used in empirical survival analysis was 21 for the Neches River and 20 for the Sabine River.

Empirical survival analysis

The best model of individual detection probability for the Neches River incorporated a shared detection probability (Table 3). There was little support for effects of site (ΔDIC = 80), species (ΔDIC > 1,000) or time (ΔDIC > 2,400) on detection probability. The median detection probability across sites, species, and sampling events was 0.816 (95% CRI = (0.795-0.839; Figure 2). We used this detection model as a starting point to investigate changes in survival during the second phase of model selection.

The best supported survival model for freshwater mussels in the Neches River included site-, species-, and time-specific survival probabilities across all species (Table 3). The median annual survival across species was 0.895 (95% CRI = 0.318-0.997). Median survival was 0.817 (0.290-0.996) across species in the lower Neches River (Hardin County) and was 0.927 (0.386-0.997) at the upper site (Rockland, Tyler County). Most species, including Louisiana Pigtoe and Texas Heelsplitter, closely approximated this median in the lower Neches River whereas all species did in the upper site (Figure 3). Estimated apparent survival was 0.921 (0.409-0.997) for Louisiana Pigtoe and 0.920 (0.379-0.997) for Texas Heelsplitter across sites (Table S1). Site-specific survival estimates ranged from a low of 0.378 (0.147-0.679) for Washboard (*Megalonaias nervosa*) in the lower site to a high of 0.940 (0.564-0.997) for Wartyback (*Cyclonaias nodulata*) in the lower Neches River (Data S1), whereas estimates of apparent survival for all species approximated the overall median in the upper site (Figure 3).

The best model of individual detection probability in the Sabine River included species-specific differences in detection (Table 4). There was little support for additional site-specific (ΔDIC > 300) or time-based (ΔDIC > 600) differences in detection probability. The median detection probability across species was 0.445 (95% CRI = 0.317-0.603). Median detection probability was 0.458 (0.374-0.587) for Louisiana Pigtoe and 0.447 (0.327-0.646) for Texas Heelsplitter. Detection probability ranged from a low of 0.385 (0.289-0.507) for Texas Pigtoe (*Fusconaia chunii* [*F. askewi*]) to a high of 0.466 (0.380-0.595) for Yellow Sandshell (*Lampsilis teres*; Figure 4, Table S2).

The best supported survival model for Sabine River mussels incorporated species-specific survival probabilities (Table 4). There was little additional support for site-specific survival probabilities (ΔDIC > 100). Mean apparent survival across all species during the first year was 0.747 (0.500-0.948). Estimated survival of most species was close to this median (Figure 5). Apparent survival was 0.753 (0.476-0.950) for Louisiana Pigtoe and 0.754 (0.448-0.952) for Texas Heelsplitter across sites (Table S3). Survival ranged from a low of 0.678 (0.521-0.816) for Pimpleback (*Cyclonaias pustulosa*) to a high of 0.817 for Louisiana Pigtoe, Yellow Sandshell (95% CRI = 0.682-0.957), and Washboard (95% CRI = 0.675-0.970) across sites (Table S3).

Simulation-based power analysis

The accuracy and precision of estimated survival for both the Texas Heelsplitter and Louisiana Pigtoe increased with increasing sample size and number of surveys conducted. Estimated apparent survival was biased low for both species at sample sizes of less than approximately 100 individuals, after which error was unbiased (Figure 6). Precision of estimated survival decreased across all sample sizes considered, but standard deviation of estimated survival was minimized with 10 sampling periods (Figure 7). In keeping with these trends, the mean squared error of estimates for both species was minimized at approximately 100 individuals across all sampling periods considered (Figure 8).

Synthesis

We were able to produce preliminary estimates of individual detection probability and apparent annual survival for a wide range of freshwater mussel species in multiple rivers in Texas, USA. Individual detection probabilities varied among rivers in this study and was variable among species within the Sabine River. We found that survival was generally high across species in the Neches River, though it was evident that some species lacked sufficient data to produce precise estimates. Survival in the Sabine River mussel populations was generally lower than in the Neches River, although survival was better estimated for a larger number of species present therein. Due to the limited number of individuals tagged for most species, additional study is needed to accurately and precisely estimate population demographic parameters.

The results of the simulation-based power analysis provide a useful tool for designing future studies. Trends in bias and precision of apparent survival estimates suggest that increased duration of sampling within the Neches and Sabine rivers would improve both accuracy and precision of estimates for individual species. In the Neches River, estimated apparent survival of focal species (Louisiana Pigtoe and Texas Heelsplitter) was high relative to the Sabine River. This was consistent for most species and is due to a combination of small sample sizes and timing of initial tagging. Less common species (Tables 1 and 2) generally tended to have apparent survival estimates that were higher and more closely approximated posterior medians (Figures 3 and 5). Increased numbers of resampling events could improve estimates of apparent survival for those less common species that were not collected the second or third sampling events in the present study.

Many, less common species also were not collected until the second sampling event (Data S1). However, inference about survival was necessarily restricted to the first sampling interval in empirical analyses because apparent survival in the final interval is confounded with detection probability in the terminal sampling event. Simulation results suggest that the accuracy and precision of these estimates could be improved through additional surveys, and where possible, larger sample sizes of mussels. Few species in either river met the minimum sample sizes (~100 individuals) that the power analysis indicated was necessary for accurate and precise estimates. In the absence of larger sample sizes, additional surveys would improve accuracy and precision and the hierarchical modeling framework employed here would allow improved sharing of information across species.

These estimates provide a baseline to be able to determine any future changes to freshwater mussel survival and detection probabilities. For some species, these represent the first attempts to empirically estimate survival in a field setting. The information gained about these species can be used to design single- or multi-species studies in the future to further improve understanding of freshwater mussel population dynamics.

References

Box, J. B., R. M. Dorazio, and W. D. Liddell. 2002. Relationships between streambed substrate characteristics and freshwater mussels (Bivalvia:Unionidae) in coastal plain streams. Journal of the North American Benthological Society 21:253–260.

Cormack, R. M. (1964). Estimates of Survival from the Sighting of Marked Animals. Biometrika, 51(3/4), 429–438. https://doi.org/10.2307/2334149

Gelman, A., and D. B. Rubin. 1992. Inference from iterative simulation using multiple sequences. Statistical Science 7:457–472.

Gillis, P. L., J. Salerno, C. J. Bennett, Y. Kudla, and M. Smith. 2021. The relative toxicity of road salt alternatives to freshwater mussels: Examining the potential risk of eco-friendly de-icing products to sensitive aquatic species. Water 1:1628–1636.

Gimenez, O., V. Rossi, R. Choquet, C. Dehais, B. Doris, H. Varella, J.-P. Vila, and R. Pradel 2007. State-space modelling of data on marked individuals. Ecological Modelling 206(3–4):431–438.

Haag, W. R. 2012. North American Freshwater Mussels. Cambridge Press.

Haag, W. R., and J. D. Williams, J. D. 2014. Biodiversity on the brink: An assessment of conservation strategies for North American freshwater mussels. Hydrobiologia 735:45–60.

Haag, W., and M. L. Warren. 1998. Role of ecological factors and reproductive strategies in structuring freshwater mussel communities. Canadian Journal of Fisheries and Aquatic Sciences 55:297–306.

Jolly, G. M. 1965. Explicit estimates from capture-recapture data with both death and immigration-stochastic model. Biometrika 52(1/2):225–247.

Kéry, M., and M. Schaub. 2012. Bayesian population analysis using WinBUGS: A hierarchical perspective. Academic Press.

Knauss, J. 2022. snowfall: Easier cluster computing (based on 'snow'). R package version 1.84-6.2. URL: https://CRAN.R-project.org/package=snowfall.

Lebreton, J.-D., K. P. Burnham, J. Clobert, J., and D. R. Anderson. 1992. Modeling survival and testing biological hypotheses using marked animals: A unified approach with case studies. Ecological Monographs 62:67–118.

Ricciardi, A., and J. B. Rasmussen. 1999. Extinction rates of North American freshwater fauna. Conservation Biology 13:1220–1222.

Royle, J. A. 2008. Modeling individual effects in the Cormack–Jolly–Seber model: A state–space formulation. Biometrics 64:364–370.

Seber, G. A. F. 1965. A note on the multiple-recapture census. Biometrika 52(1/2):249–259.

Sotola, V. A., K. T. Sullivan, B. M. Littrell, N. H. Martin, D. S. Stich, and T. H. Bonner. 2021. Short-term responses of freshwater mussels to floods in a southwestern U.S.A. river estimated using mark–recapture sampling. Freshwater Biology 66:349–361.

Strayer, D. L. 1993 Microhabitats of freshwater mussels (Bivalvia: Unionacea) in streams of the northern Atlantic Slope. Journal of the North American Benthological Society 12:236–246.

Strayer, D., D. Hunter, L. Smith, and C. Borg. 2006. Distribution, abundance, and roles of freshwater clams (Bivalvia, Unionidae) in the freshwater tidal Hudson River. Freshwater Biology 31:239–248.

Strayer, D. L., J. A. Downing, W. R. Haag, T. L. King, J. B. Layzer, T. J. Newton, and J. S. Nichols. 2004. Changing perspectives on pearly mussels, North America's most imperiled animals. BioScience 54:429–439.

Strayer, D. L., and J. Ralley. 1993. Microhabitat use by an assemblage of stream-dwelling Unionaceans (Bivalvia), including two rare species of Alasmidonta. Journal of the North American Benthological Society 12:247–258.

Williams, J. D., M. L. Warren, K. S. Cummings, J. L. Harris, and R. J. Neves. 1993. Conservation status of freshwater mussels of the United States and Canada. Fisheries 18(9):6–22.

Ziuganov, V., E. S. Miguel, R. J. Neves, A. Longa, C. Fernández, R. Amaro, V. Beletsky, E. Popkovitch, S. Kaliuzhin, S., and T. Johnson. 2000. Life span variation of the freshwater pearl shell: a model species for testing longevity mechanisms in animals. AMBIO: A Journal of the Human Environment 29(2):102–105.

Table 1. Species of freshwater mussels and number of individuals tagged from the lower and upper sites (Figure 1) in the Neches River, Texas, USA 2021-2022. One Texas Lilliput (*Toxolasma texasiense*) was collected but not tagged during the first marking period and is not counted in the table.

Scientific name	Common name	Lower	Upper
Amblema plicata	Threeridge	91	210
Arcidens confragosus	Rock Pocketbook	1	0
Cyclonaias nodulata	Wartyback	1	0
Cyclonaias pustulosa	Pimpleback	18	188
Fusconaia chunii (*Fusconaia askewi*)	Texas Pigtoe	0	12
Glebula rotundata	Round Pearlshell	119	0
Lampsilis hydiana	Louisiana Fatmucket	13	7
Lampsilis satura	Sandbank Pocketbook	1	0
Lampsilis teres	Yellow Sandshell	50	33
Megalonaias nervosa	Washboard	12	32
Obliquaria reflexa	Threehorn Wartyback	110	37
Plectomerus dombeyanus	Bankclimber	96	131
Pleurobema riddellii	Louisiana Pigtoe	0	39
Potamilus amphichaenus	Texas Heelsplitter	10	6
Potamilus fragilis	Fragile Papershell	1	11
Potamilus purpuratus	Bleufer	13	233
Pyganodon grandis	Giant Floater	5	0
Quadrula quadrula	Mapleleaf	317	13
Tritogonia nobilis	Gulf Mapleleaf	213	32
Tritogonia verrucosa	Pistolgrip	0	23
Truncilla donaciformis	Fawnsfoot	1	1
Total		1,072	1,008

Table 2. Species of freshwater mussels and number of individuals tagged at Lower and Upper sites (Figure 1) in the Sabine River, Texas, USA 2020-2022.

Scientific name	Common name	Lower	Upper
Amblema plicata	Threeridge	1	1
Arcidens confragosus	Rock Pocketbook	1	15
Cyclonaias pustulosa	Pimpleback	56	179
Fusconaia chunii (*Fusconaia askewi*)	Texas Pigtoe	313	111
Lampsilis hydiana	Louisiana Fatmucket	0	2
Lampsilis satura	Sandbank Pocketbook	6	44
Lampsilis teres	Yellow Sandshell	56	45
Megalonaias nervosa	Washboard	19	29
Obliquaria reflexa	Threehorn Wartyback	22	50
Plectomerus dombeyanus	Bankclimber	0	13
Pleurobema riddellii	Louisiana Pigtoe	0	179
Potamilus amphichaenus	Texas Heelsplitter	3	5
Potamilus fragilis	Fragile Papershell	22	5
Potamilus purpuratus	Bleufer	29	22
Quadrula quadrula	Mapleleaf	44	191
Strophitus undulatus	Creeper	0	5
Tritogonia verrucosa	Pistolgrip	124	188
Truncilla truncata	Deertoe	6	52
Utterbackia imbecillis	Paper Pondshell	7	0
Villosa (*Leaunio*) *lienosa*	Little Spectaclecase	0	1
Total		709	1137

Table 3. Deviance Information Criterion (DIC) statistics for Cormack-Jolly-Seber mark-recapture models of freshwater mussel survival in the Neches River, Texas, USA 2021-2022. The letter *t* denotes temporal differences, *s* denotes species-specific differences, and *j* represents site-specific differences. Model selection for candidate detection models was conducted prior to fitting alternate model structures to the apparent survival parameter. All models in the Neches River included time-specific survival rates because intervals between sampling events were variable. The lower the DIC the better the model within each set. Models with ΔDIC < 2.0 have similar support within the candidate set.

Model set	Model	DIC	ΔDIC
Detection	$\varphi_. p_.$	6025	0
	$\varphi_. p_j$	6105	80
	$\varphi_. p_s$	7607	1582
	$\varphi_. p_{tsj}$	8009	1984
	$\varphi_. p_t$	8514	2489
	$\varphi_. p_{ts}$	8547	2522
	$\varphi_. p_{tj}$	8605	2580
Survival	$\varphi_{tsj} p_.$	8352	0
	$\varphi_{ts} p_.$	8787	435
	$\varphi_t p_.$	9188	836
	$\varphi_{tj} p_.$	9712	1360

Table 4. Deviance Information Criterion (DIC) statistics for Cormack-Jolly-Seber mark-recapture models of freshwater mussel survival in the Sabine River, Texas, USA 2020-2022. Symbols and abbreviations are defined as in Table 3.

Model set	Model	DIC	ΔDIC
Detection	$\varphi.p_{s}$	7108	0
	$\varphi.p.$	7504	396
	$\varphi.p_{j}$	7885	777
	$\varphi.p_{tj}$	7992	884
	$\varphi.p_{t}$	8182	1074
	$\varphi.p_{tsj}$	8856	1748
	$\varphi.p_{ts}$	10186	3078
Survival	$\varphi_{ts}p_{s}$	7248	0
	$\varphi_{tsj}p_{s}$	7371	123
	$\varphi_{s}p_{s}$	7373	125
	$\varphi_{js}p_{s}$	7517	269
	$\varphi_{j}p_{s}$	8277	1029
	$\varphi_{tj}p_{s}$	8849	1601
	$\varphi_{t}p_{s}$	9114	1867

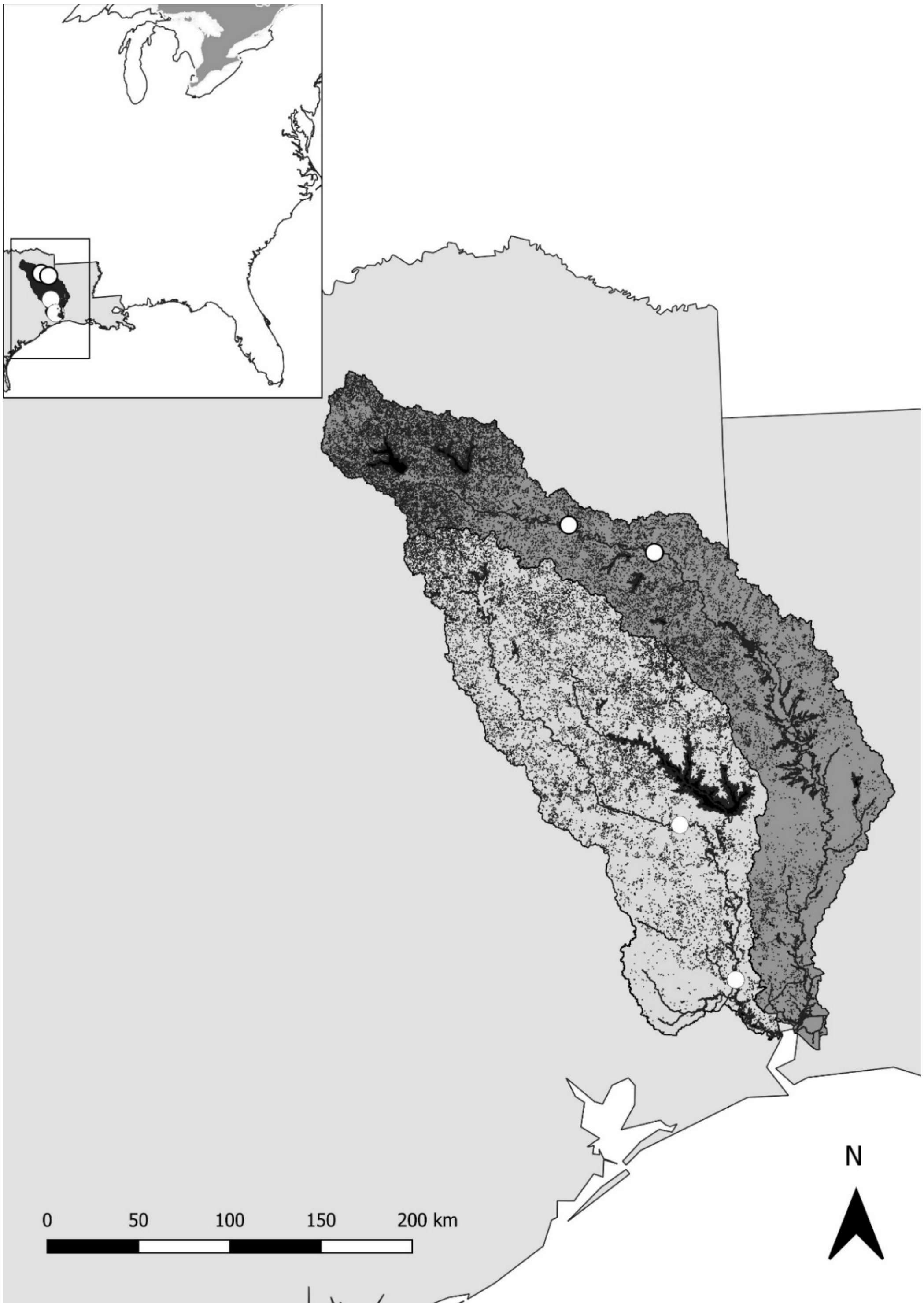

Figure 1. Map showing the Neches River watershed (light gray) and Sabine River watershed (gray) and their location in Texas, USA (inset). White dots are sampling locations in each river, with "lower" sampling sites being closer to the coast in each system.

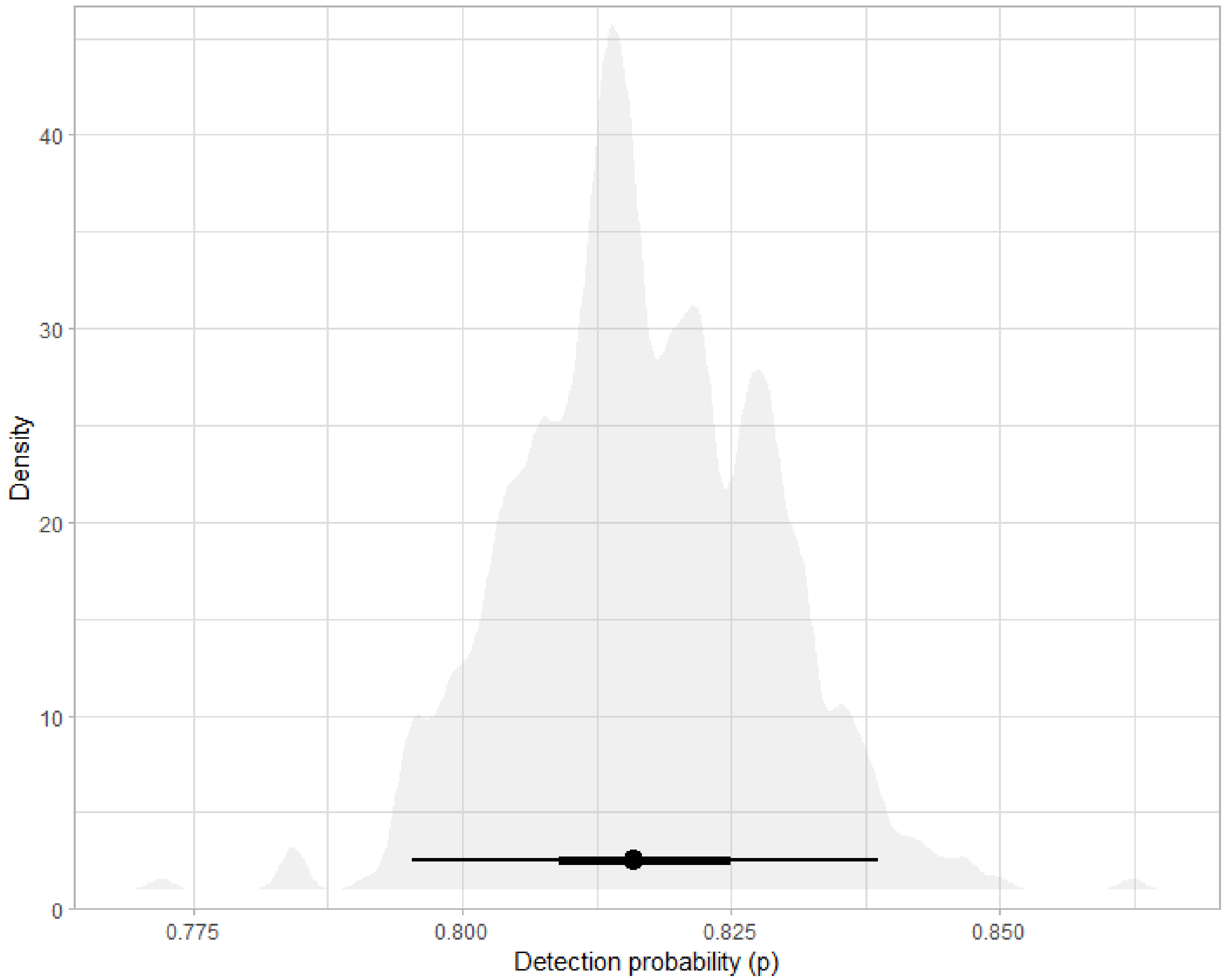

Figure 2. Posterior density of estimated detection probability across 2 sites and 22 species of freshwater mussels 2021-2022 in the Neches River Texas, USA. The gray polygon is the posterior density for detection probability, points are posterior medians, thick horizontal lines are interquartile range (25th and 75th percentile), and thin horizontal lines are 95% credible intervals.

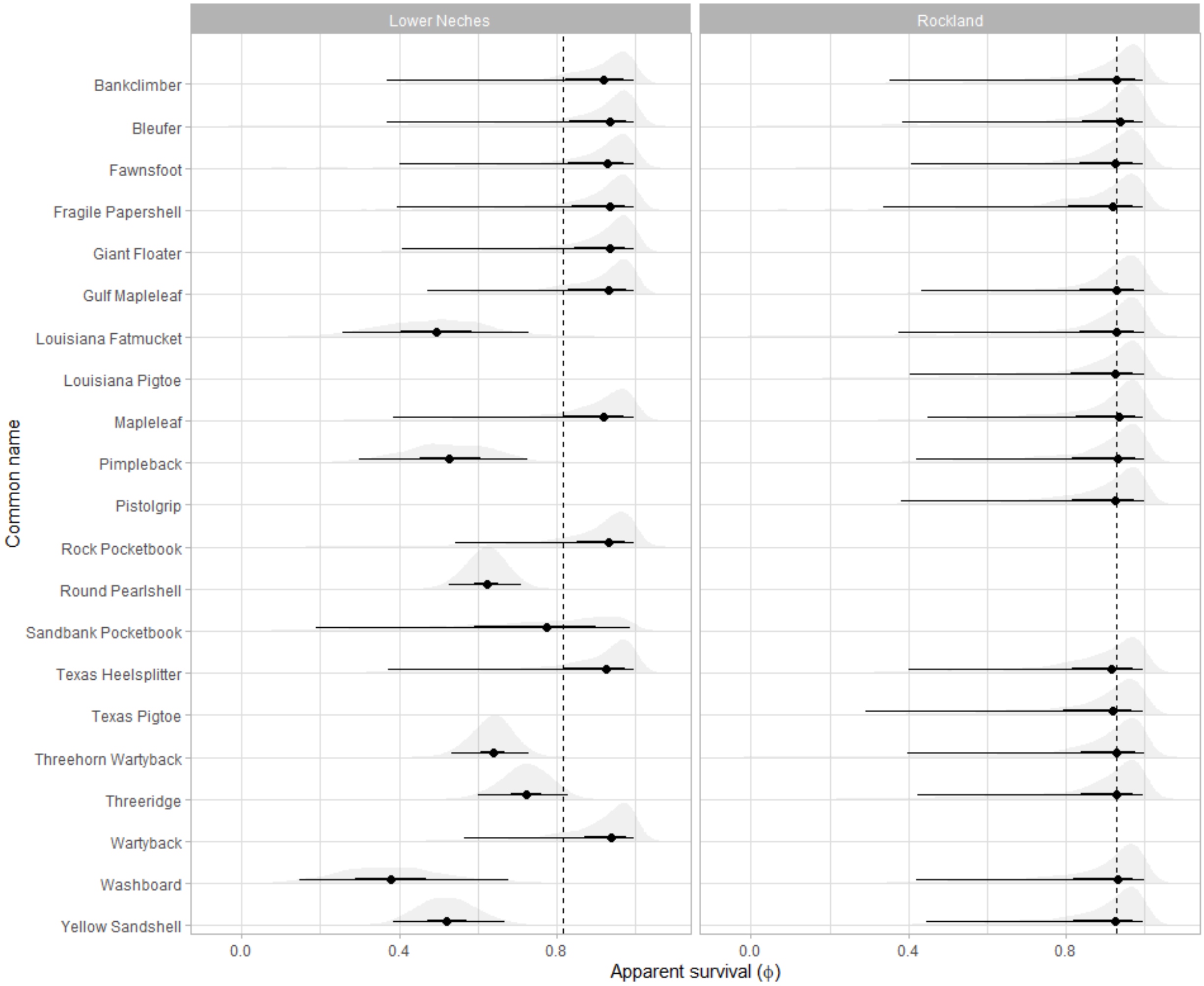

Figure 3. Species-specific apparent survival estimates for 21 species of freshwater mussels 2021-2022 in the Neches River Texas, USA. Symbols are defined as in Figure 2. Species not detected at a given site are blank.

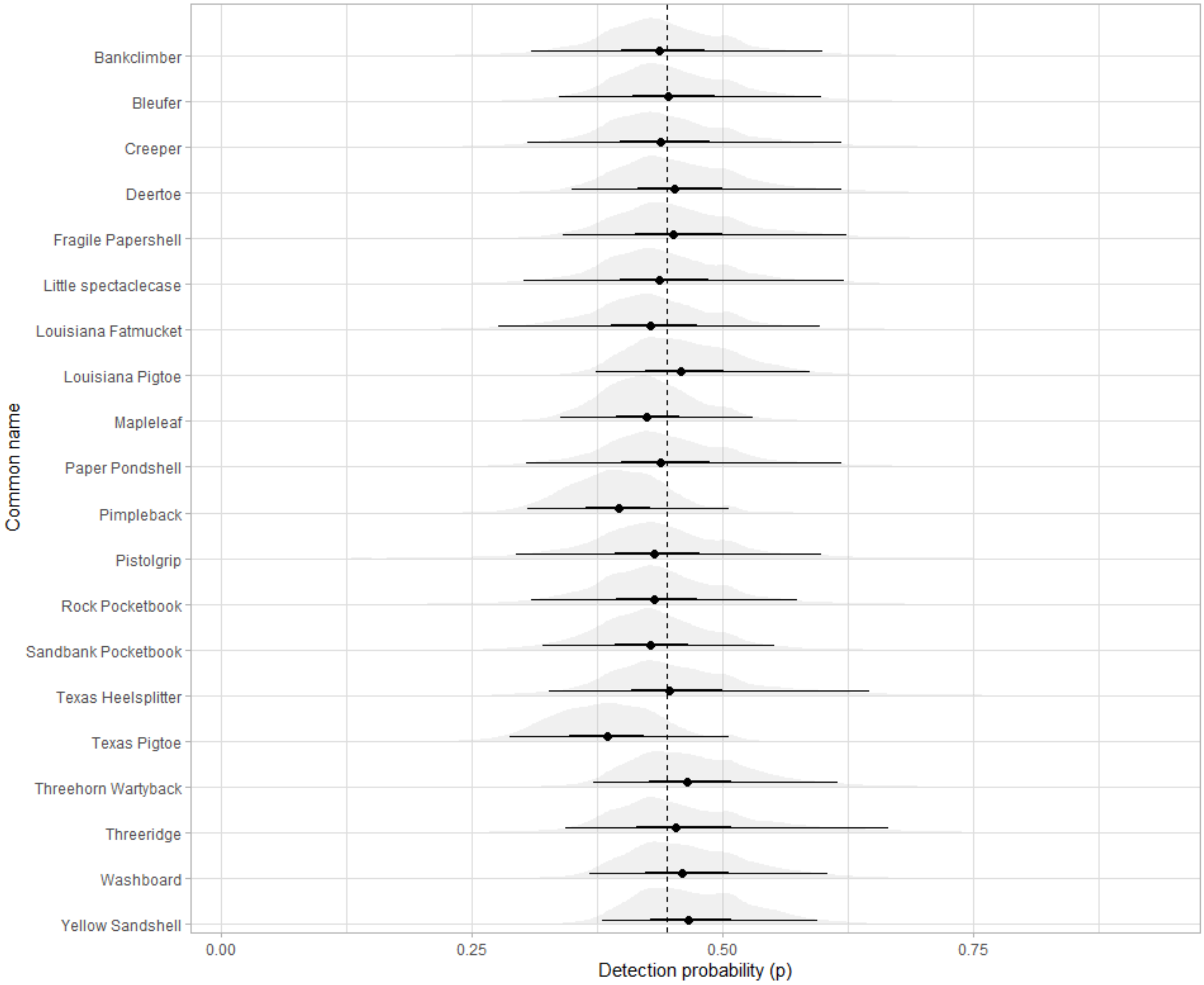

Figure 4. Species-specific, posterior distributions of detection probabilities for 20 species of freshwater mussels 2020-2022 in the Sabine River Texas, USA. Symbols are defined as in Figures 2.

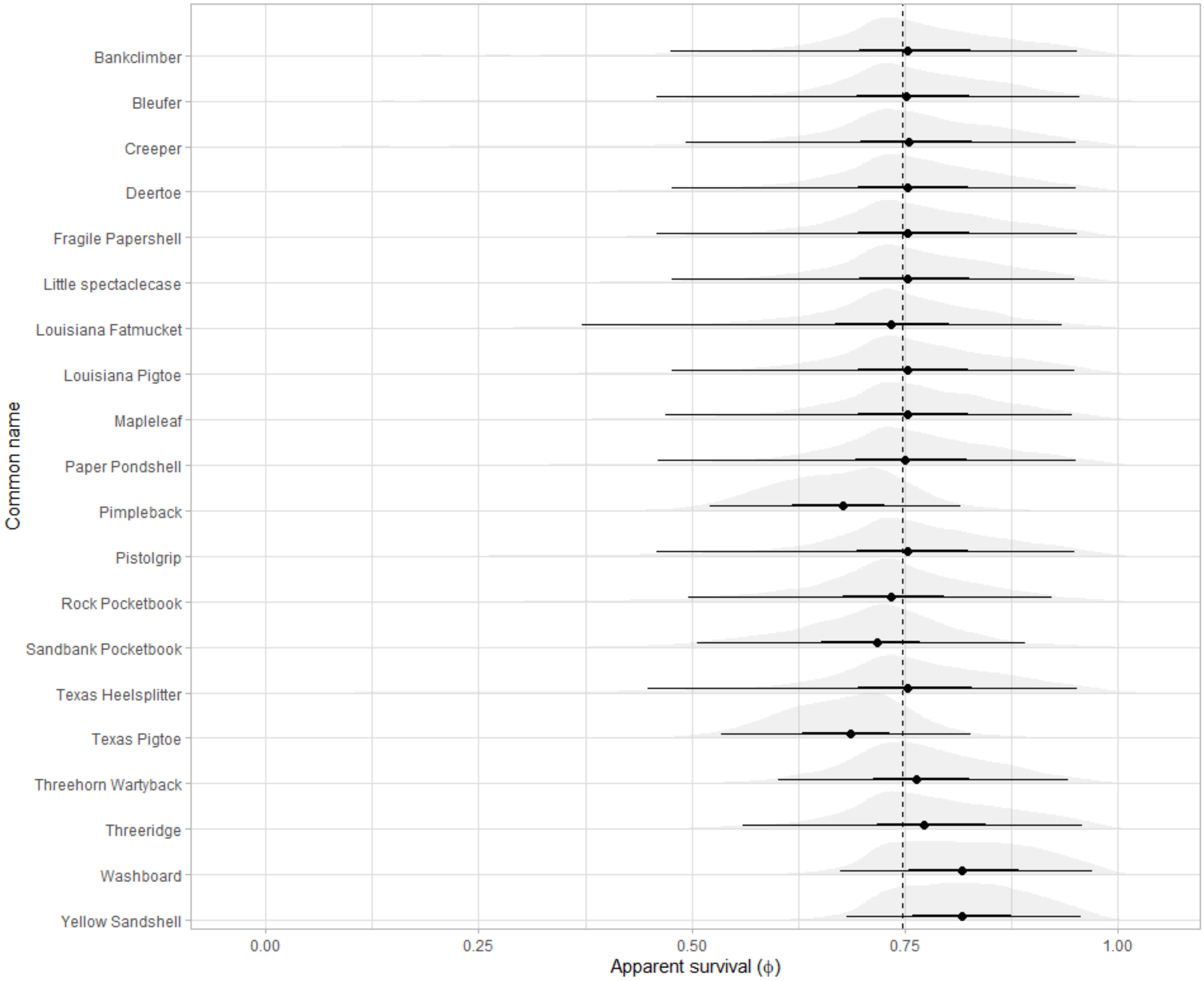

Figure 5. Species-specific, posterior distributions of apparent survival (φ) for 20 species of freshwater mussels in the Sabine River, Texas, USA 2020-2021. Symbols are defined as in Figure 2.

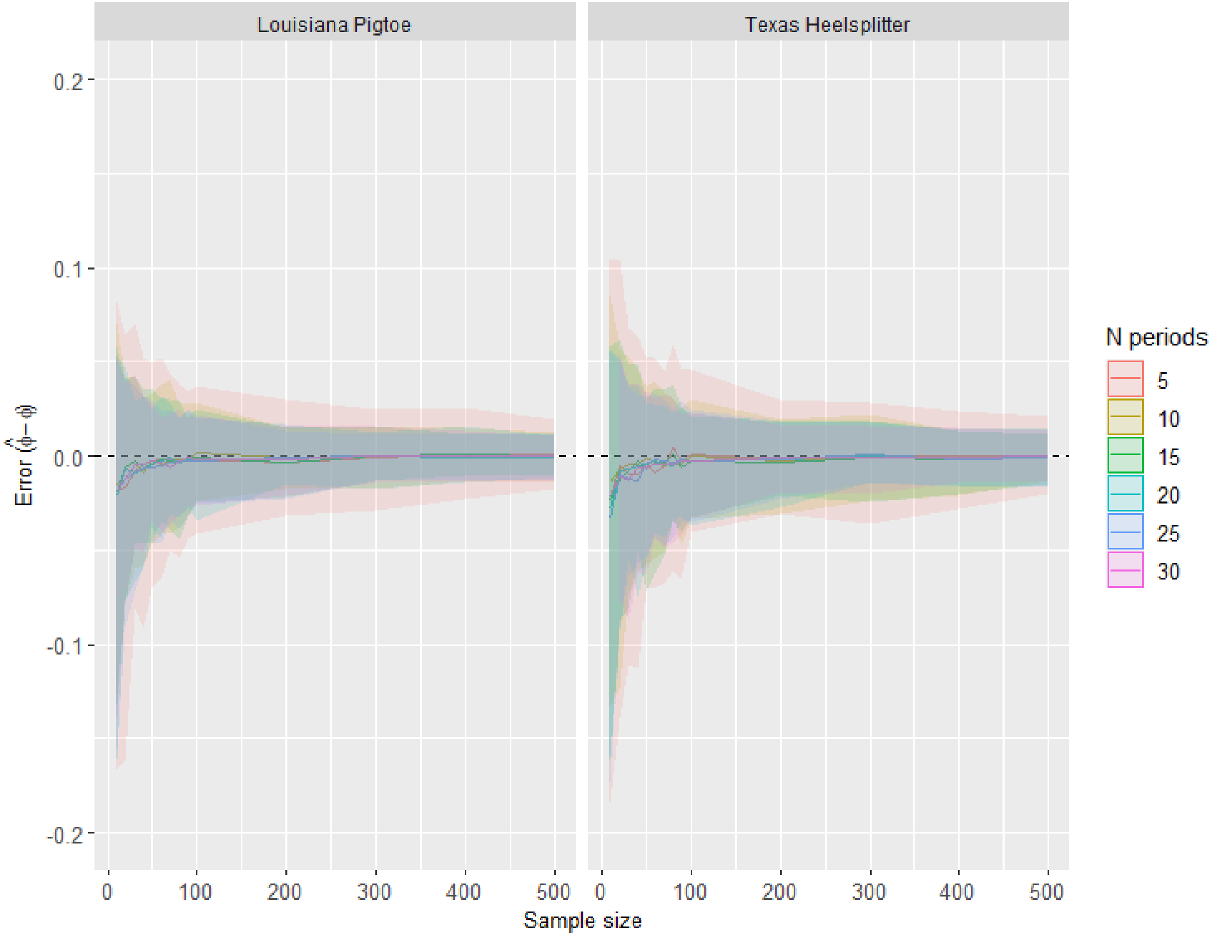

Figure 6. Bias of estimated apparent annual survival of Texas Heelsplitter (*Potamilus amphichaenus*) and Louisiana Pigtoe (*Pleurobema riddellii*) as a function of number of individuals tagged (Sample size) and number of sampling events (N periods). The solid lines represent mean error from simulation-based power analysis and the colored ribbons are bootstrapped 95% confidence intervals.

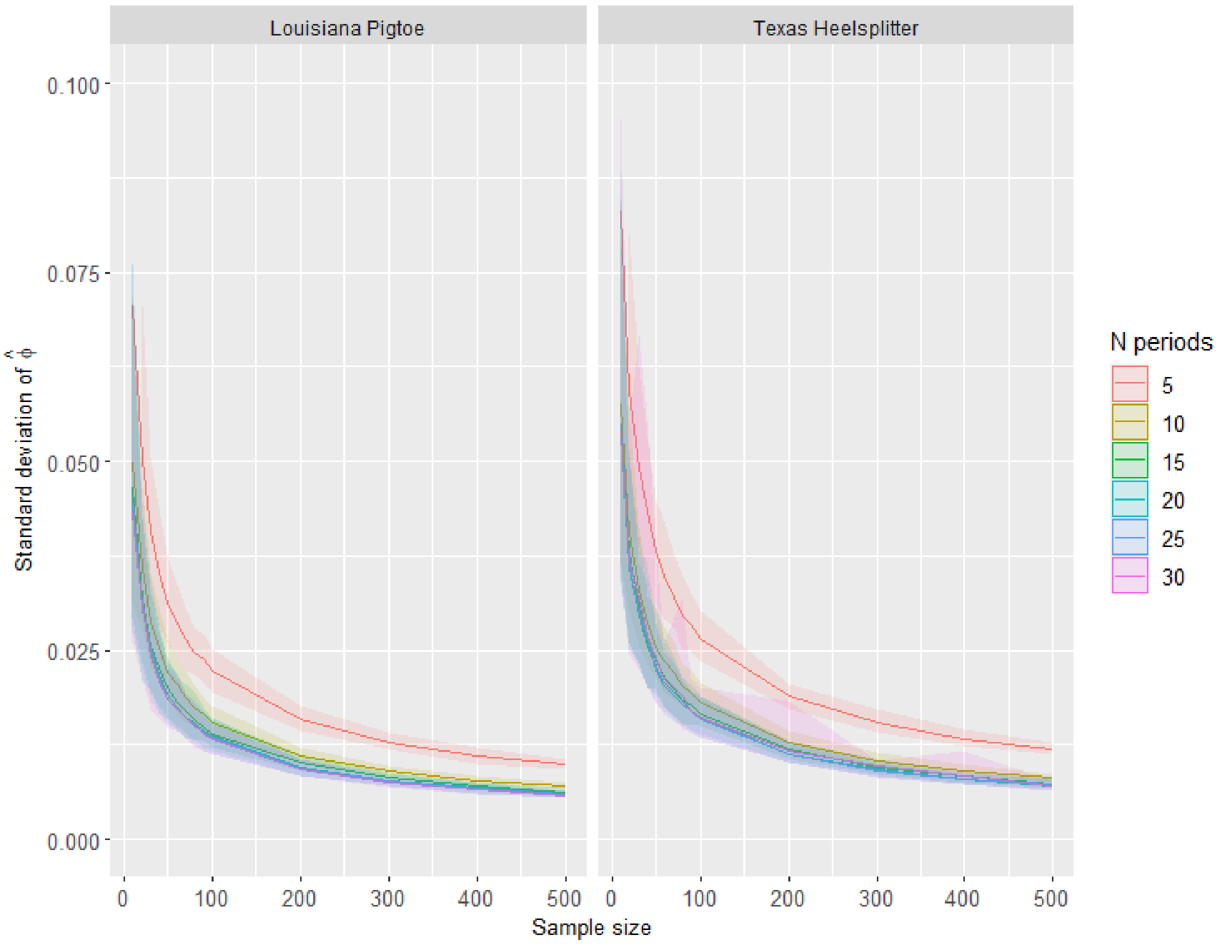

Figure 7. Precision of estimated apparent annual survival of Texas Heelsplitter (*Potamilus amphichaenus*) and Louisiana Pigtoe (*Pleurobema riddellii*) as a function of number of individuals tagged (Sample size) and number of sampling events (N periods). The solid lines represent mean bias from simulation-based power analysis and the colored ribbons are bootstrapped 95% confidence intervals.

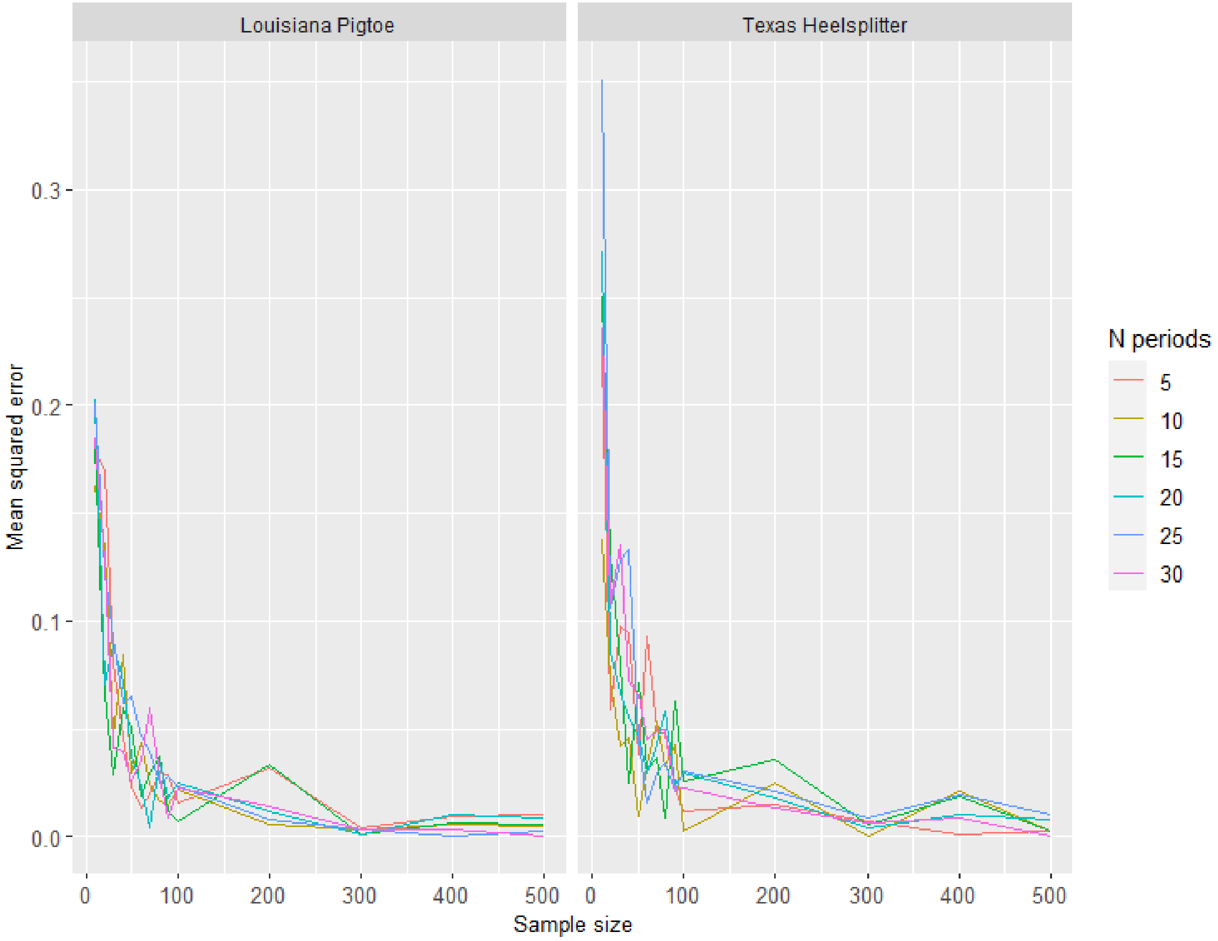

Figure 8. Mean squared error (MSE) of estimated apparent annual survival of Texas Heelsplitter (*Potamilus amphichaenus*) and Louisiana Pigtoe (*Pleurobema riddellii*) as a function of number of individuals tagged (Sample size) and number of sampling events (N periods). The solid lines represent mean bias from simulation-based power analysis.

Supplemental Data

Data S1. Data and code used for empirical survival analysis and simulation-based power analysis are available through GitHub: https://github.com/danStich/mussels.

Table S1. Species-specific estimates of apparent annual survival for 16 species of freshwater mussels 2021-2022 in the Neches River, Texas, USA, showing posterior median, standard deviation (S.D.) and upper and lower limits of 95% credible intervals.

Scientific name	Common name	Median	Lower	Upper
Amblema plicata	Threeridge	0.775	0.526	0.995
Arcidens confragosus	Rock Pocketbook	0.935	0.460	0.997
Cyclonaias nodulata	Wartyback	0.933	0.437	0.997
Cyclonaias pustulosa	Pimpleback	0.661	0.323	0.996
Fusconaia chunii (*Fusconaia askewi*)	Texas Pigtoe	0.920	0.321	0.997
Glebula rotundata	Round Pearlshell	0.676	0.508	0.995
Lampsilis hydiana	Louisiana Fatmucket	0.643	0.272	0.994
Lampsilis satura	Sandbank Pocketbook	0.863	0.259	0.995
Lampsilis teres	Yellow Sandshell	0.627	0.395	0.994
Megalonaias nervosa	Washboard	0.585	0.172	0.994
Obliquaria reflexa	Threehorn Wartyback	0.693	0.488	0.995
Plectomerus dombeyanus	Bankclimber	0.925	0.351	0.997
Pleurobema riddellii	Louisiana Pigtoe	0.921	0.409	0.997
Potamilus amphichaenus	Texas Heelsplitter	0.920	0.379	0.997
Potamilus fragilis	Fragile Papershell	0.926	0.375	0.997
Potamilus purpuratus	Bleufer	0.935	0.370	0.997
Pyganodon grandis	Giant Floater	0.931	0.383	0.997
Quadrula quadrula	Mapleleaf	0.928	0.398	0.997
Tritogonia nobilis	Gulf Mapleleaf	0.930	0.447	0.997
Tritogonia verrucosa	Pistolgrip	0.923	0.363	0.997
Truncilla donaciformis	Fawnsfoot	0.927	0.402	0.997

Table S2. Species-specific estimates of individual detection probability for 20 species of freshwater mussels 2020-2022 in the Sabine River, Texas, USA, showing posterior median, standard deviation (S.D.) and upper and lower limits of 95% credible intervals.

Scientific name	Common name	Median	Lower	Upper
Amblema plicata	Threeridge	0.453	0.344	0.666
Arcidens confragosus	Rock Pocketbook	0.432	0.309	0.575
Cyclonaias pustulosa	Pimpleback	0.396	0.306	0.507
Fusconaia chunii (*Fusconaia askewi*)	Texas Pigtoe	0.385	0.289	0.507
Lampsilis hydiana	Louisiana Fatmucket	0.428	0.276	0.597
Lampsilis satura	Sandbank Pocketbook	0.428	0.321	0.551
Lampsilis teres	Yellow Sandshell	0.466	0.380	0.595
Megalonaias nervosa	Washboard	0.460	0.367	0.605
Obliquaria reflexa	Threehorn Wartyback	0.464	0.371	0.615
Plectomerus dombeyanus	Bankclimber	0.437	0.309	0.600
Pleurobema riddellii	Louisiana Pigtoe	0.458	0.374	0.587
Potamilus amphichaenus	Texas Heelsplitter	0.447	0.327	0.646
Potamilus fragilis	Fragile Papershell	0.451	0.341	0.624
Potamilus purpuratus	Bleufer	0.445	0.337	0.599
Quadrula quadrula	Mapleleaf	0.424	0.339	0.531
Strophitus undulatus	Creeper	0.438	0.305	0.619
Tritogonia verrucosa	Pistolgrip	0.432	0.295	0.599
Truncilla truncata	Deertoe	0.452	0.350	0.619
Utterbackia imbecillis	Paper Pondshell	0.438	0.304	0.619
Villosa (*Leaunio*) *lienosa*	Little spectaclecase	0.437	0.301	0.622

Table S3. Species-specific estimates of apparent annual survival for 20 species of freshwater mussels 2020-2022 in the Sabine River, Texas, USA, showing posterior median, standard deviation (S.D.) and upper and lower limits of 95% credible intervals.

Species name	Common name	Median	Lower	Upper
Amblema plicata	Threeridge	0.772	0.560	0.958
Arcidens confragosus	Rock Pocketbook	0.734	0.495	0.923
Cyclonaias pustulosa	Pimpleback	0.678	0.521	0.816
Fusconaia chunii	Texas Pigtoe	0.686	0.535	0.827
(Fusconaia askewi)				
Lampsilis hydiana	Louisiana Fatmucket	0.734	0.372	0.935
Lampsilis satura	Sandbank Pocketbook	0.717	0.507	0.892
Lampsilis teres	Yellow Sandshell	0.817	0.682	0.957
Megalonaias nervosa	Washboard	0.817	0.675	0.970
Obliquaria reflexa	Threehorn Wartyback	0.763	0.602	0.942
Plectomerus dombeyanus	Bankclimber	0.753	0.475	0.952
Pleurobema riddellii	Louisiana Pigtoe	0.753	0.476	0.950
Potamilus amphichaenus	Texas Heelsplitter	0.754	0.448	0.952
Potamilus fragilis	Fragile Papershell	0.753	0.459	0.952
Potamilus purpuratus	Bleufer	0.751	0.459	0.956
Quadrula quadrula	Mapleleaf	0.754	0.470	0.946
Strophitus undulatus	Creeper	0.755	0.493	0.951
Tritogonia verrucosa	Pistolgrip	0.754	0.460	0.949
Truncilla truncata	Deertoe	0.754	0.477	0.950
Utterbackia imbecillis	Paper Pondshell	0.751	0.460	0.951
Villosa (*Leaunio*) *lienosa*	Little spectaclecase	0.753	0.477	0.949

Task 3. Population genetics analysis of *P. riddellii*

Contributing Authors: Alex Zalmat, Matthew Harrison, Brad Littrell, Tim Bonner, Noland Martin

Addresses:
Texas State University, Department of Biology, San Marcos, Texas 78666 (AZ, MH, TB, NM)
BIO-WEST, Inc. San Marcos Texas 78666 (BL)

Principal Investigators: Noland Martin and Tim Bonner

Email: noland.martin@txstate.edu and TBonner@txstate.edu

Study objectives

The objectives were 1) to assess genetic structure of *P. riddellii* across their reported range, 2) to evaluate whether genetic structure is influenced spatially, including potential barriers to gene flow and whether it varies between major river drainages and environmental associations, and 3) to assess if genetic structure is characterized by recognizable sub-populations within river systems.

Methods

Collection and DNA library preparation

In order to assess genetic structure of *P. riddellii*, we collected tissue samples from and phenotypically identified *P. riddellii* in the Neches, Sabine, Calcasieu, Red, Ouachita, and Pearl river basins from 2019-2020. A second collection effort was made in 2022-2023 to increase the geographic coverage of this dataset, which added the Calcasieu drainage to the *P. riddellii* collection, and the Big Cypress and Bayou Pierre localities (Red River basin) to the *Fusconaia* collections. We simultaneously collected and sequenced individuals from several other species of Unionid mussels that share range overlap with *P. riddellii*, including *Cyclonaias pustulosa, Quadrula quadrula, Tritogonia nobilis, Fusconaia chunii, Fusconaia flava, Leptodea fragilis,* and *Potamilus amphichaenus* to assess the confidence of our nominal species designations made in the field. In total, 321 *P. riddellii* were collected and analyzed in the context of this larger Unionid species collection (total dataset n = 692), with *P. riddellii* collections summarized in Table 1. In total, two DNA sequence libraries were generated, one from each collection period. These libraries were then combined to perform all subsequent analyses presented here.

Genetic assembly and analysis

Two genetic assemblies were generated: one using the larger Unionid dataset, and one using only individuals identified as *P. riddellii* in the species-level analysis. The large "global" Unionid assembly that included all 692 individuals from across all species mentioned above was used to assess genetic variation across and within species in the dataset using Principal Component Analysis (PCA). This first assembly allowed us to identify individuals that were mis-identified in the field using only phenotype, and to either include them or exclude them as appropriate from further analyses/assemblies. Once individuals were confirmed as *P. riddellii,* they were included in the *P. riddellii*-specific assembly, which was subsequently used to investigate finer-scale geographic patterns of genetic variation within the *P. riddellii* collection, as described in the objectives outlined above.

Results

Global multi-species assembly results

PCA largely resolved nominal species-level differences in the large multi-species dataset, with PC axes 1 and 2 explaining 48.1% and 10.85% of the variance, respectively (Figure 1). PC axis 1 distinguishes *C. pustulosa, T. nobilis* and *Q. quadrula, L. fragilis*, and *P. riddellii* from each other, while PC axis 2 separated the *Fusconaia* species (Figure 1). PC axis 3 (2.95% of variance explained) then cleanly separated *F. flava* from *F. chunii* (Figure 2). Interestingly PC3 also separates *P. riddellii* in the Calcasieu drainage from other *P. riddellii* populations (see objectives 1 and 2). Another interesting finding is that an individual mis-identified in the field as *F. flava* sampled from Bayou Pierre in the Red River basin clustered with *P. riddellii* (Figure 2-cluster A). This would place genetically confirmed *P. riddellii* in a locality where the species was thought to have been recently extirpated. A third *P. riddellii* cluster forms along PC3, which we suggest is likely explained by differences in coverage between the two separately prepared DNA libraries. Differences in coverage depth between the two libraries potentially result in false signals of genetic divergence at this scale.

Figure 2 demonstrates this effect by designating clusters based on which library the samples were prepped in. Library A represents the 2019-2020 collection, while Library B represents the most recently prepared collection (Figures 2-4). These two libraries differ in terms of sequence coverage depth, with individuals in Library A having on average half the coverage of individuals from Library B (Figure 3). This phenomenon is known to occur when datasets of differing coverage are combined, and we are currently working on several solutions to resolve this issue which are described in more detail below. It should be noted that when we cannot rule out coverage differences or low sample size as explanations for clustering in PC space, clusters may have biological relevance, although further rigorous analysis is required to support this. Once the coverage difference issues are resolved, we will continue with further analyses that will clarify the findings made here.

P. riddellii assembly results

The *P. riddellii*-specific PCA yielded some clustering, resolving the Neches and Calcasieu basins (Figure 4, clusters A and B respectively). Big Cypress (Red River basin) also forms a cluster (cluster D in Figure 4), although low coverage cannot be ruled out as this cluster entirely belongs to the lower coverage Library A. Cluster C in Figure 4 represents the bulk of Library A individuals, and as can be seen from the multiple basins represented in this single large cluster, this cluster is likely unresolved due to in being entirely made up of Library A individuals and thus having lower coverage. It should also be noted that clusters A and C in Figure 4 share some geographic localities, and as such should theoretically have some individuals clustering together by locality. Given that these clusters separate out entirely by library alone suggests that this pattern is driven by coverage differences between the two libraries. PC axis 1 (12.83% variance explained) appears to separate the two libraries and therefore coverage differences in the data may be loading heavily onto this axis. PC axis 2 (5.05% variance explained) appears to give us more biologically relevant clusters, however the coverage issue must be addressed before full-scale population structure can be assessed. It should be noted that Library A on its own did show some differentiation by drainage basin, and that differentiation should still be present in the dataset once the coverage differences are resolved (Harrison, 2022).

Future Directions

The analysis of population genetic structure and variation is ongoing, and additional analyses are needed to fully explore the patterns within *P. riddellii*. Before moving forward with more robust population genetic analyses, the issues generated from differences in coverage between the two DNA libraries mentioned above must be dealt with. Several solutions to this issue are being worked on and include: 1) subsampling loci that have high coverage in Library A and then re-running the analysis with those loci selected for all individuals, 2) assembling all the *P. riddellii* data to the original de-novo reference sequence generated when Library A was first worked up, and 3) partitioning out the variance associated with coverage differences from the genotype likelihoods and then performing the PCA with the corrected data.

Once this coverage issue has been dealt with, more fine scale population genetic analyses will be performed on the data. We plan to use a hierarchical Bayesian model known as Entropy (Gompert et al. 2014) to assess fine scale population structure and to identify potential areas of gene flow. We also plan to use F statistics commonly used in population genetic studies to corroborate any findings in previous analyses. Estimates of genetic diversity and environmental association models will also be used to assess patterns of genetic variation. The information generated from this work will then be synthesized into a manuscript and submitted for publication.

References

Gompert, Z., L. K. Lucas, C. A. Buerkle, M. L. Forister, J. A. Fordyce, and C. C. Nice. 2014. Admixture and the organization of genetic diversity in a butterfly species complex revealed through common and rare genetic variants. Molecular Ecology 23: 4555–4573.

Harrison, M. Population Genetic Structure of Unionid Mussels Across Multiple Gulf Drainages. Masters Thesis, Texas State University, San Marcos, TX, USA, 2022.

Table 1-*P. riddellii* collections included in the larger genetic dataset. Collections are organized by basin and then by river within basin. *Bayou Dorcheat represents the only locality in the study that did not yield *P. riddellii*. “PCA cluster” refers to which cluster in the *P. riddellii*-specific PCA (Figure 4) individuals from each locality grouped with.

Basin	River	N	PCA Cluster
San Jacinto	San Jacinto	37	A,B
Neches	Angelina	9	C
	Neches	164	A,C
Sabine	Sabine	39	C
Calcasieu	Calcasieu	37	A
Red	Big Cypress	12	D
	Bayou Dorcheat*	0	
	Bayou Pierre	1	A
	Little River	16	C
Ouachita	Ouachita	4	C
Pearl		2	C
	Total	321	

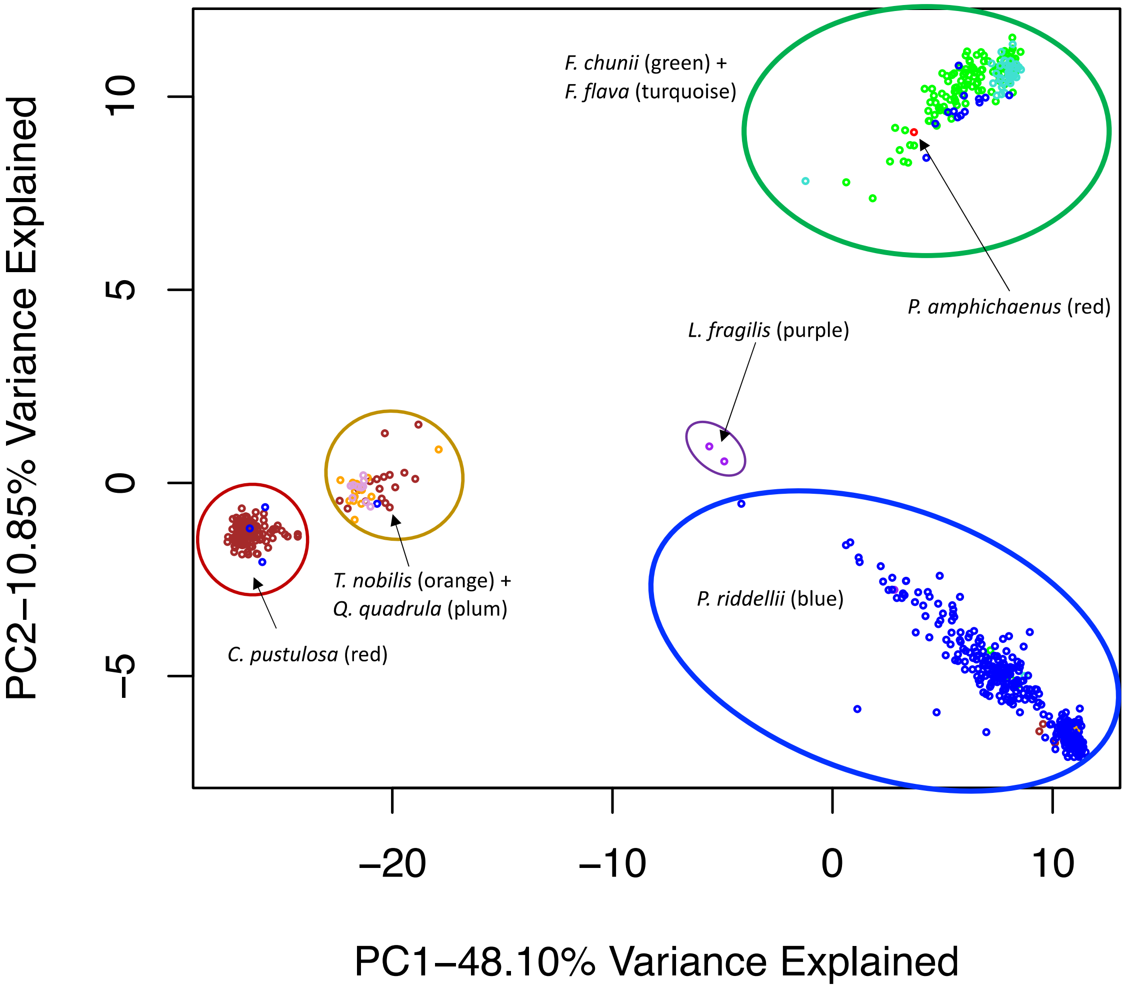

Figure 1. PCA plot of genotype likelihoods showing PC axes 1 and 2 of the global assembly. Each point represents an individual, which are colored by nominal field species identification. Clusters of the same color represent appropriately identified individuals, while points that have a different color than the cluster in which they appear represent misidentifications. Clusters are circled and labeled by species.

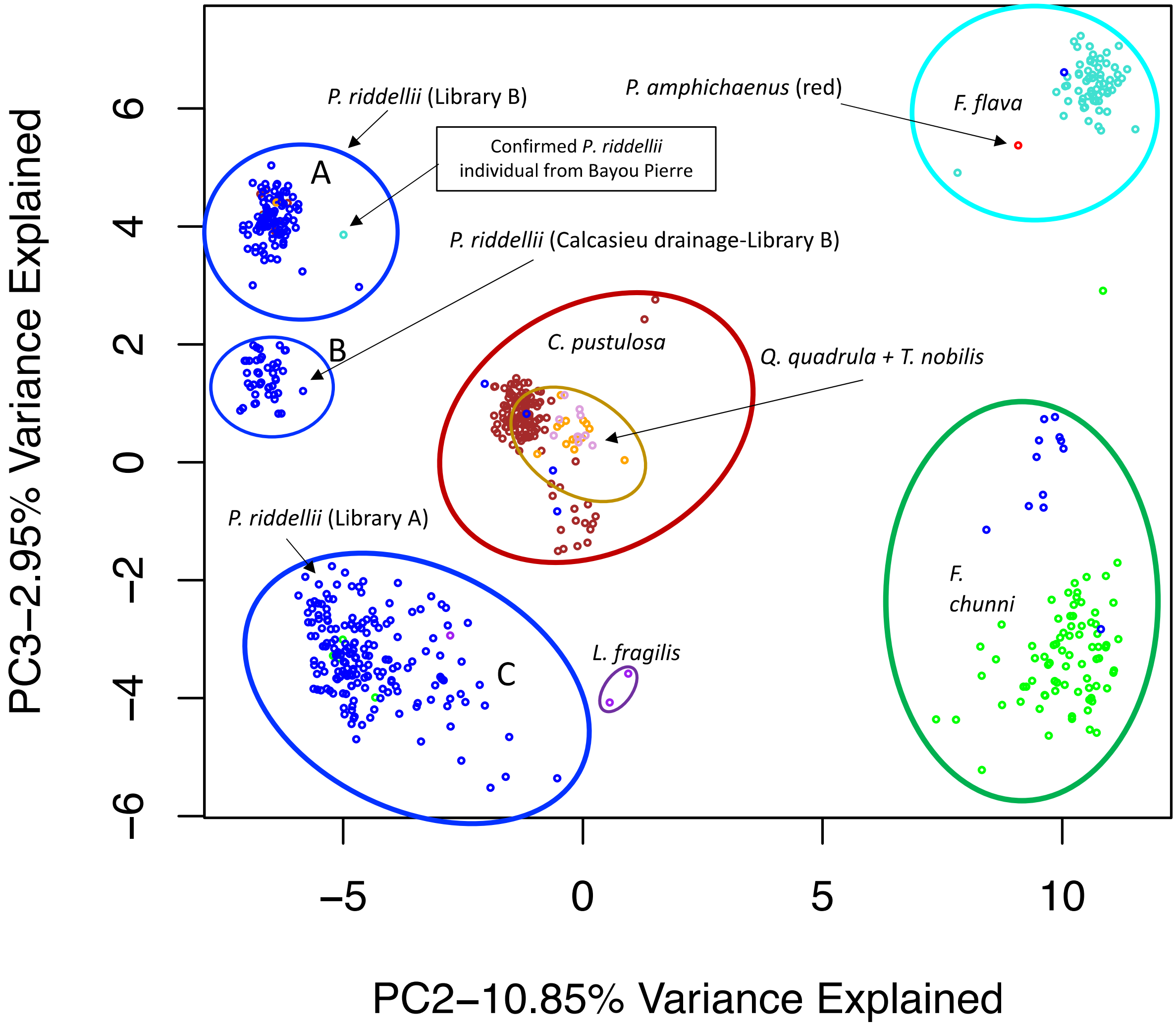

Figure 2. PCA plot of genotype likelihoods showing PC axes 2 and 3 of the global assembly. Each point represents an individual, which are colored by nominal field species identification. Clusters of the same color represent appropriately identified individuals, while points that have a different color than the cluster in which they appear represent misidentifications. Clusters are circled and labeled by species. The 3 *P. riddellii* clusters are also labeled by library (either A or B) to show the coverage-difference effect.

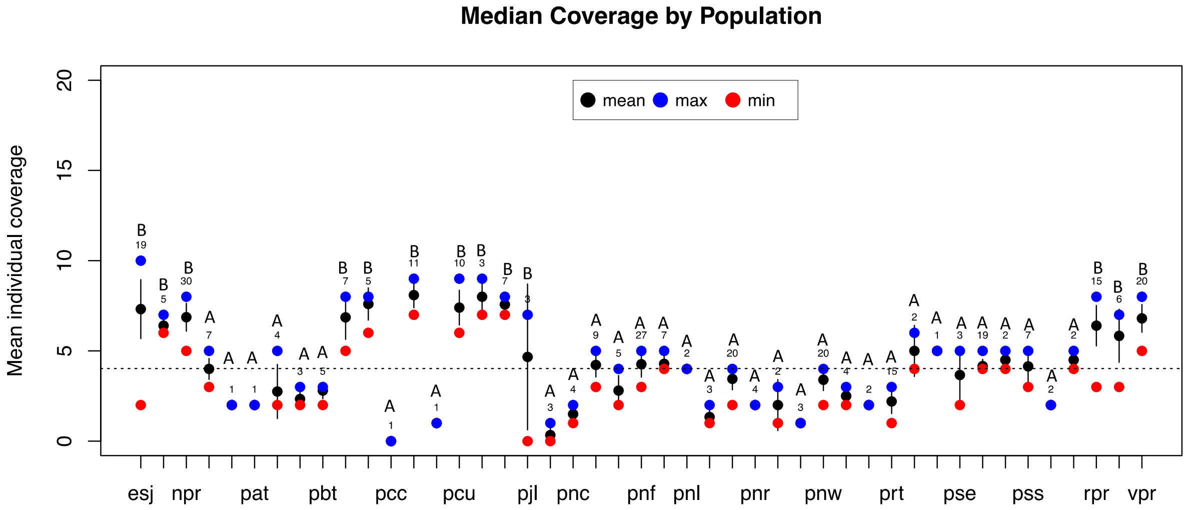

Figure 3. Median coverage by collection locality showing whether the collection was included in Library A or Library B (letters above each point). Library B had on average approximately half the coverage of Library A.

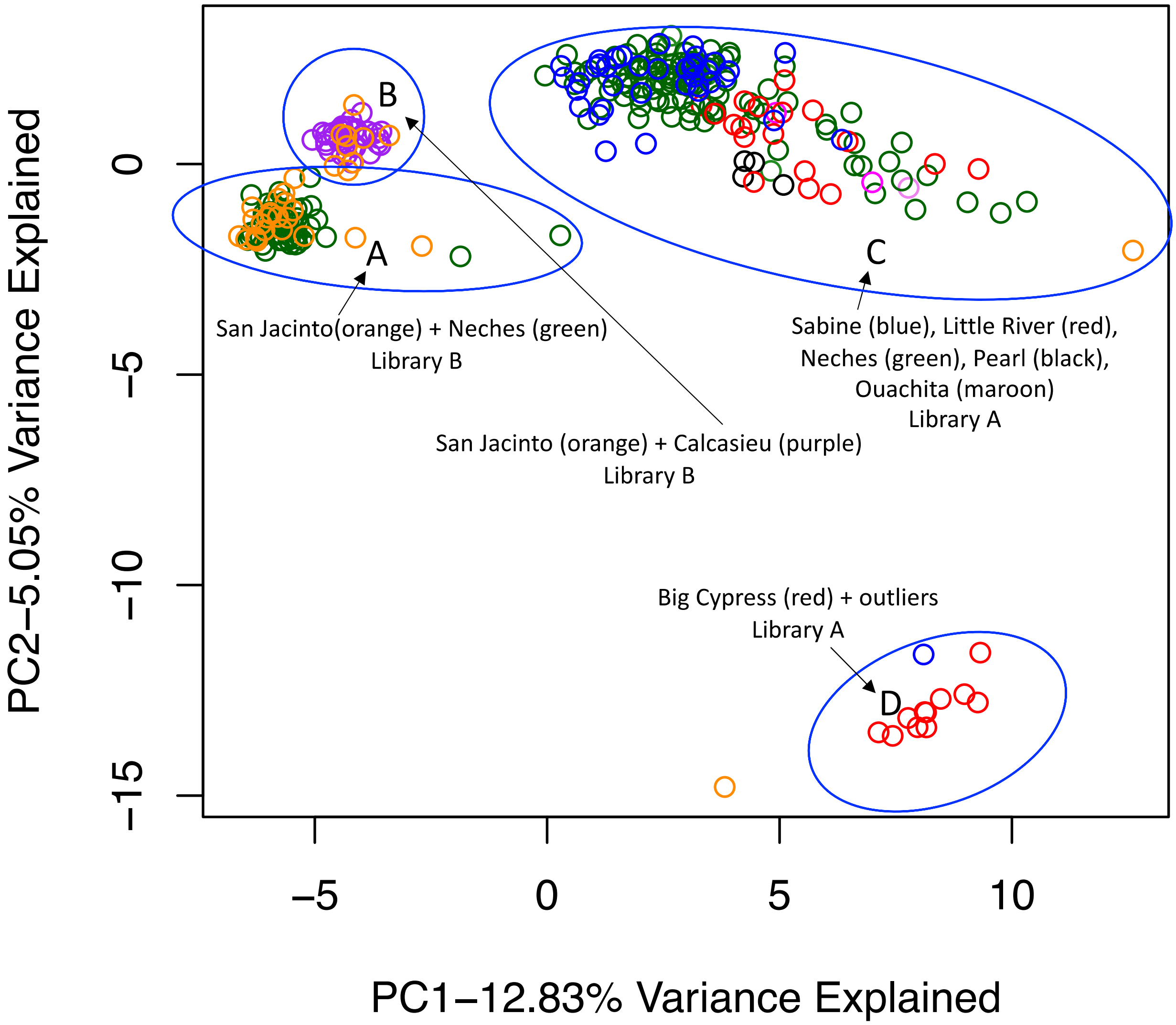

Figure 4. PCA plot of genotype likelihoods showing PC axes 1 and 2 of the *P. riddellii* assembly. Each point represents an individual, which are colored by drainage basin of collection. Clusters are circled and labeled by basin and by the library they were prepped from (A or B). 4 clusters are suggested which are labeled A through D.